Volume 10, Issue 18 – January – June – 2023

ECORFAN

Journal-Bolivia

ISSN-On line: 2410-4191

ECORFAN®

ECORFAN Journal-Bolivia, Volume 10, Issue 18, June - 2023, is a biannual Journal edited by ECORFAN-Bolivia and the international academy. Santa Lucia N-21, Barrio Libertadores, Cd. Sucre. Chuquisaca, Bolivia, http://www.ecorfan.org/bolivia/journal.php, journal@ecorfan.org. Editor in charge: Fernando Iglesias-Suarez, MsC ISSN: 2410-4191. Responsible for the last update of this issue ECORFAN Computer Unit. Imelda Escamilla Bouchán, PhD. Vladimir Luna Soto, PhD. Santa Lucia N-21, Barrio Libertadores, Cd. Sucre. Chuquisaca, Bolivia. Date of last update June 30, 2023.

ECORFAN-Journal Bolivia

Definition of the Journal

Scientific Objectives

Support the international scientific community in its written production Science, Technology and Innovation in the Field of Medicine and Health Sciences, in Subdisciplines Engineering, Chemical, Optical, Resources, Food technology, Anatomy, Nutrition.

ECORFAN-Mexico, S.C. is a Scientific and Technological Company in contribution to the Human Resource training focused on the continuity in the critical analysis of International Research and is attached to CONAHCYT-RENIECYT number 1702902, its commitment is to disseminate research and contributions of the International Scientific Community, academic institutions, agencies and entities of the public and private sectors and contribute to the linking of researchers who carry out scientific activities, technological developments and training of specialized human resources with governments, companies and social organizations.

Encourage the interlocution of the International Scientific Community with other Study Centers in Mexico and abroad and promote a wide incorporation of academics, specialists and researchers to the publication in Science Structures of Autonomous Universities - State Public Universities - Federal IES - Polytechnic Universities - Technological Universities - Federal Technological Institutes - Normal Schools - Decentralized Technological Institutes - Intercultural Universities - S & T Councils - CONAHCYT Research Centers.

Scope, Coverage and Audience

ECORFAN -Journal Bolivia is a Journal edited by ECORFAN-Mexico S.C in its Holding with repository in Bolivia, is a scientific publication arbitrated and indexed with semester periods. It supports a wide range of contents that are evaluated by academic peers by the Double-Blind method, around subjects related to the theory and practice of Engineering, Chemical, Optical, Resources, Food technology, Anatomy, Nutrition with diverse approaches and perspectives , That contribute to the diffusion of the development of Science Technology and Innovation that allow the arguments related to the decision making and influence in the formulation of international policies in the Field of Medicine and Health Sciences. The editorial horizon of ECORFAN-Mexico® extends beyond the academy and integrates other segments of research and analysis outside the scope, as long as they meet the requirements of rigorous argumentative and scientific, as well as addressing issues of general and current interest of the International Scientific Society.

Editorial Board

Arbitration Committee

Assignment of Rights

The sending of an Article to ECORFAN -Journal Bolivia emanates the commitment of the author not to submit it simultaneously to the consideration of other series publications for it must complement the Originality Format for its Article.

The authors sign the Authorization Format for their Article to be disseminated by means that ECORFAN-Mexico, S.C. In its Holding Bolivia considers pertinent for disclosure and diffusion of its Article its Rights of Work.

Declaration of Authorship

Indicate the Name of Author and Coauthors at most in the participation of the Article and indicate in extensive the Institutional Affiliation indicating the Department.

Identify the Name of Author and Coauthors at most with the CVU Scholarship Number-PNPC or SNI-CONAHCYT- Indicating the Researcher Level and their Google Scholar Profile to verify their Citation Level and H index.

Identify the Name of Author and Coauthors at most in the Science and Technology Profiles widely accepted by the International Scientific Community ORC ID - Researcher ID Thomson - arXiv Author ID - PubMed Author ID - Open ID respectively.

Indicate the contact for correspondence to the Author (Mail and Telephone) and indicate the Researcher who contributes as the first Author of the Article.

Plagiarism Detection

All Articles will be tested by plagiarism software PLAGSCAN if a plagiarism level is detected Positive will not be sent to arbitration and will be rescinded of the reception of the Article notifying the Authors responsible, claiming that academic plagiarism is criminalized in the Penal Code.

Arbitration Process

All Articles will be evaluated by academic peers by the Double Blind method, the Arbitration Approval is a requirement for the Editorial Board to make a final decision that will be final in all cases. MARVID® is a derivative brand of ECORFAN® specialized in providing the expert evaluators all of them with Doctorate degree and distinction of International Researchers in the respective Councils of Science and Technology the counterpart of CONAHCYT for the chapters of America-Europe-Asia- Africa and Oceania. The identification of the authorship should only appear on a first removable page, in order to ensure that the Arbitration process is anonymous and covers the following stages: Identification of the Journal with its author occupation rate - Identification of Authors and Coauthors - Detection of plagiarism PLAGSCAN - Review of Formats of Authorization and Originality-Allocation to the Editorial Board-Allocation of the pair of Expert Arbitrators-Notification of Arbitration -Declaration of observations to the Author-Verification of Article Modified for Editing-Publication.

Instructions for Scientific, Technological and Innovation Publication

Knowledge Area

The works must be unpublished and refer to topics of Engineering, Chemical, Optical, Resources, Food technology, Anatomy, Nutrition and other topics related to Medicine and Health Sciences.

Presentation of the Content

In the first chapter we present, *Structural and optical properties of metal-organic frameworks of lanthanides*, by MEDINA-AMBRIZ, Alan Raúl, LOERA-SERNA, Sandra, ALARCON-FLORES, Gilberto and AGUILAR-FRUTIS, Miguel Ángel, with ascription in the Universidad Autónoma Metropolitana and Instituto Politécnico Nacional, as a second article we present, *Development and physicochemical evaluation of a snail protein-based worcestershire sauce (Helix aspersa)*, by REYNOSO-OCAMPO, Carlos Abraham, ARROYO-CRUZ, Celerino and TREJO-TREJO, Elia, with secondment in the Universidad Tecnológica del Valle del Mezquital, as the following article we present, *Chromate resistance in Cupriavidus metallidurans CH34: molecular modeling from ChrC superoxide* dismutase, by DÍAZ-PÉREZ, Alma Laura, CASTRO-MORENO, Patricia, VELOZ-GARCÍA, Rafael Alejandro and DÍAZ-PÉREZ, César, with affiliation at the Universidad Michoacana de San Nicolás de Hidalgo, Universidad Nacional Autónoma de México and Universidad de Guanajuato, as next article we present, *Nephroprotection of p-coumaric acid against sublethal dose of carbon tetrachloride in Wistar rats: histological evidence*, by MACÍAS-PÉREZ, José Roberto, ALDABA-MURUATO, Liseth Rubí, HERNÁNDEZ-MARTÍNEZ, Jazmín Guadalupe and SÁNCHEZ-BRIONES, María Eugenia, with affiliation at the Universidad Autónoma de San Luis Potosí.

Content

Article **ECORFAN Journal-Bolivia**
June 2023, Vol.10 No.18 1-9

Structural and optical properties of metal-organic frameworks of lanthanides

Propiedades estructurales y ópticas de redes metal orgánicas de lantánidos

MEDINA-AMBRIZ, Alan Raúl†´, LOERA-SERNA, Sandra*´, ALARCON-FLORES, Gilberto*´´ and AGUILAR-FRUTIS, Miguel Ángel´´

´ *Universidad Autónoma Metropolitana, Azcapotzalco, CDMX, México.*
´´ *Instituto Politécnico Nacional (IPN), Centro de Investigación en Ciencia Aplicada y Tecnología Avanzada (CICATA), CDMX, México.*

ID 1st Author: *Alan Raúl, Medina-Ambriz* / **ORC ID:** 0009-0009-0753-8309, **CVU CONAHCYT ID:** 1232456

ID 1st Co-author: *Sandra, Loera-Serna* / **ORC ID:** 0000-0001-9562-3195, **CVU CONAHCYT ID:** 172467

ID 1st Co-author: *Gilberto, Alarcon-Flores* / **ORC ID:** 0000-0002-4094-524X **CVU CONAHCYT ID:** 170047

ID 1st Co-author: *Miguel Ángel, Aguilar-Frutis* / **ORC ID:** 0000-0002-2651-0936, **CVU CONAHCYT ID:** 18768

DOI: 10.35429/EJB.2023.18.10.1.9 Received January 10, 2023; Accepted June 30, 2023

Abstract

In this work, the synthesis of luminescent metal-organic frameworks (LnMOF) was studied at room temperature using different lanthanides ions as metal centers. LnMOFs are materials that can emit light by absorbing energy from other radiation and have been used mainly as sensors in medicine, optics, electronics, and the chemical industry. The synthesis was carried out by stirring at room temperature and with a stoichiometry of 1:1, using trimesic acid as an organic linker. Structural characterization of these materials was carried out using DRX, FT-IR, and SEM. Synthesis of isoreticular MOFs with Eu, Tb, Dy, Nd, and Er with crystal sizes between 24-64 nm was possible. Regarding the optical properties, these were determined by photoluminescence spectroscopy. The MOFs that presented intense emission and excitation bands were those of Eu, Tb, and Dy, being the most intense of Tb. With the results obtained, it is possible to obtain 3D luminescent MOFs using a simple and easy methodology, which does not involve high-frequency processes such as ultrasound or microwaves, or post-synthesis procedures, which are very frequent and considerably increase the synthesis time or the expense of solvents for material washings but above all a high energy consumption.

Frameworks; emission; lanthanides

Resumen

En este trabajo se estudió la síntesis de marcos metalorgánicos luminiscentes (LnMOF) a temperatura ambiente utilizando diferentes iones lantánidos como centros metálicos. Los LnMOFs son materiales que pueden emitir luz absorbiendo energía de otras radiaciones y se han utilizado principalmente como sensores en medicina, óptica, electrónica e industria química. La síntesis se llevó a cabo por agitación a temperatura ambiente y con una estequiometría de 1:1, utilizando ácido trimésico como enlazador orgánico. La caracterización estructural de estos materiales se llevó a cabo mediante DRX, FT-IR y SEM. Fue posible la síntesis de MOFs isoreticulares con Eu, Tb, Dy, Nd, y Er con tamaños de cristal entre 24-64 nm. En cuanto a las propiedades ópticas, éstas se determinaron mediante espectroscopia de fotoluminiscencia. Los MOFs que presentaron bandas de emisión y excitación intensas fueron los de Eu, Tb, y Dy, siendo la más intensa la de Tb. Con los resultados obtenidos, es posible obtener MOFs luminiscentes 3D mediante una metodología sencilla y fácil, que no implica procesos de alta frecuencia como ultrasonidos o microondas, ni procedimientos post-síntesis, que son muy frecuentes y aumentan considerablemente el tiempo de síntesis o el gasto de disolventes para el lavado del material pero sobre todo un elevado consumo energético.

Estructuras, Emisión, Lantánidos

Citation: MEDINA-AMBRIZ, Alan Raúl, LOERA-SERNA, Sandra, ALARCON-FLORES, Gilberto and AGUILAR-FRUTIS, Miguel Ángel. Structural and optical properties of metal-organic frameworks of lanthanides. ECORFAN Journal-Bolivia. 2023. 10-18:1-9.

* Correspondence to Author (E-mail: sls@azc.uam.mx, galarcon@ipn.mx)
† Researcher contributing first author.

Introduction

Metal-organic frameworks (MOF) or coordination polymers are a solid porous material with a crystalline structure formed by a metallic cluster and an organic ligand [Rocío-Bautista, 2019] to form one-dimensional, two-dimensional or three-dimensional structures [Porcher, *et al*., 2000]. Among its properties, it stands out that depending on the nature of the components, they present a high chemical and thermal stability, they are materials with large and uniform porosities, up to 90% of the volume is free, these materials have the largest internal surface area in their structure, which gives rise to values that extend beyond 6000 m^2/g [Farha, *et al*., 2012]. All these characteristics make MOFs suitable for use in extraction processes, gas storage, catalysis, and sensors [Rocío-Bautista, 2019].

Speaking of the structure of organic metal frameworks, it can be said that these are crystalline where the lattice points are metallic centers and the links of the structure are the organic ligands, which are also the union bridges between the metallic ions [Pérez Carrasco, et al., 2020]. In this type of structure, the organic binder gives more flexibility and topology diversity to the frameworks. The ligands used in the synthesis of MOF are conjugated organic compounds that, due to their chromophoric characteristics and the interactions of the conjugated bonds with their environment, absorb in the UV-Visible region and acquire structural rigidity in the framework [Rocío-Bautista, 2019].

MOFs can be synthesized using an element that generates MOFs with luminescent properties (LnMOF) as a metal center. In the case of LnMOF, the ions of metal atoms that are commonly used to produce visible light are some transition metals such as chromium (Cr) and manganese (Mn) or ions belonging to the lanthanide family [Garduño-Wilches, et al., 2021]. There are several methods for obtaining LnMOF, the best known being the solvothermal method, the ultrasound method and the microwave-assisted solvothermal method.

LnMOFs are not similar to inorganic complexes, this is due to their symmetrical pores and large surface area. The differences between these two types of materials are due to the absorption of photons by the organic binder, the transfer of energy from the organic binder to the activating center within the organic metal lattice. (antenna effect), the emission of the activator when going from the excited state to the ground state and the rigidity imposed by the ligand constrain the position of the lanthanides in a different way from that observed in inorganic compounds.

In addition, several different mechanisms have been reported by which an LnMOF can present luminescence: emission from the organic ligand, metal-linker transfer, linker-metal transfer, emission promoted by the host molecule [Ríos Carvajal, 2014].

There are many methodologies for the synthesis of MOFs and in some cases different structures can be obtained from the same reaction. Thus, each methodology can have an impact in terms of reaction times, yields, particle size and morphology [Medina-Velázquez, et al., 2016]. Among the different methods there are three main groups: conventional synthesis methods, high-performance methods and alternative synthesis routes [Cárdenas Saavedra, 2019]. In some cases a method can be both high throughput and alternative, so this classification is not entirely suitable for synthetic methods.

The aforementioned methods correspond to unconventional synthesis because they have the following requirements: 1) A lot of energy is needed to carry out LnMOF, which significantly increases the synthesis costs, 2) Solvents such as DMF are used in the processes for obtaining LnMOF or DEF which are highly toxic. Specific conditions are required for the synthesis (vacuum or high pressure) and long times to maintain said conditions. Due to the above, processes are sought that can replace the existing ones or optimize in some way the energy requirements to obtain the LnMOF.

ISSN-On line: 2410-4191.

In this project I carry out an alternative synthesis that involves the use of room temperature. In order to be able to obtain LnMOFs in a more environmentally friendly way, that is, avoiding the use of toxic solvents, as well as excessive energy due to the use of sophisticated techniques. The LnMOFs were synthesized from some ions of the lanthanide series such as: europium (Eu^{3+}), dysprosium (Dy^{3+}), neodymium (Nd^{3+}), terbium (Tb^{3+}) and erbium (Er^{3+}). A 1:1 molar ratio of organic ligand and metal precursor, respectively, was used in the synthesis. The physicochemical characteristics of the obtained samples were determined by X-ray diffraction (XRD), Fourier transform infrared spectroscopy (FT-IR), scanning electron microscopy (SEM) and photoluminescence measurements were performed to determine the optical properties.

Methodology

Materials

The reagents were supplied by Sigma-Aldrich and were of analytical grade, used without prior purification processes and are the following: $EuCl_3 \cdot 6H_2O$ (99%), $TbCl_3 \cdot 6H_2O$ (99%), $Nd(NO_3)_3 \cdot 6H_2O$ (99%), $DyCl_3 \cdot 6H_2O$ (99%), $ErCl_3 \cdot 6H_2O$ (99%), 1,3,5-benzenetricarboxylic acid (95%), and absolute ethanol (99%).

Synthesis of MOFs

The molar ratios were the same for each solid, 1.0 mmol of the organic binder dissolved in water and 0.5 mmol of the metal precursor dissolved in ethanol were used [Alarcón-Flores, *et al.*, 2015]. Both solutions were mixed dropwise at room temperature and kept stirring for 12 h. The mixture was separated by centrifugation for 30 minutes at 6000 rpm and dried in an oven at 100 ºC, finally the solid was stored for further characterization.

Results

MOF structural properties

Figure 1 shows the X-ray diffraction patterns of the samples obtained with Nd, Dy, Eu, Tb and Er. It is observed that the peaks are at the same Bragg angle positions as the theoretical diffractogram.

The latter corresponds to a reported MOF with gadolinium and the organic ligand BTC, with a tetragonal arrangement and a space group P 43 2 2, the reported framework parameters are a=b=10.3548 Å and c= 14.5872 Å [Wang, H. 2017]. The methodology used in the synthesis of Gd-BTC included the addition of hydrochloric acid and DMF, the synthesis was carried out at 80 ºC for 12 h. In this work, the synthesis was carried out at room temperature and no acid precursor was required. In the same article, the synthesis was carried out using europium and terbium, obtaining isoreticular structures of gadolinium. Additionally, a change in the relative intensities of the peaks is observed, indicating a crystallinity that depends on the metal center used in the synthesis. To obtain a quantitative analysis, calculations of lattice parameters and crystal sizes, the results are presented in Table 1. It is observed that the calculated lattice parameters are lower in all the MOFs obtained compared to the value reported for Gd-BTC, this result can be attributed to two phenomena: i) the change in the ionic radius of the lanthanides and ii) the contraction of the structure due to the absence of solvent molecules in the pores. To rule out the contraction of the structure due to the ionic radius, the values [Sánchez, R. M.] were investigated and these are presented in Table 1, it is observed that the trend that has the decrease in the value of a0 and c0 are not equivalent to the change of the ionic radius, this indicates that the structure is isoreticular, as already mentioned, and that the ionic radius does not directly interfere with the size of the unit cell. In this sense, it is more probable that the change is due to the affinity of the metallic centers with the water molecules, this will be corroborated by the FT-IR analysis.

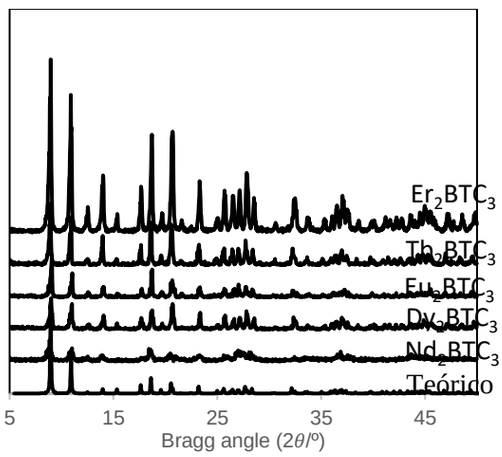

Figure 1 X-ray diffraction of the BTC samples

ISSN-On line: 2410-4191.

The crystal size obtained by the Deby-Scherrer equation (Table 1) corresponds to a nanometric material, with a smaller size for the Nd_2BTC_3 sample (24.15 nm), it seems that it obeys the larger ionic radius (1.249 Å) and the larger of 63.25nm for Eu_2BTC_3. That can be attributed to the large difference in atomic mass (7.72 amu) between Nd and Eu. The MOFs obtained with Dy, Tb and Er have a similar size close to 40 nm, most probably due to their similar ionic radius (1.167, 1.180 and 1.144 Å respectively, see Table 2). The crystal size is related to the amplitude of the peaks, so it is observed that the synthesis methodology is the one that determines the crystallinity of the material.

The most soluble cations and similar to polar solvents are those that they can be easily incorporated into the framework, through the methodology used, since in his way the solubility of the reagents is favored.

LnMOF	a(Å)	c(Å)	D(nm)
Teoric (Gd_2BTC_3)	10.35	14.59	-
Nd_2BTC_3	10.00	13.46	24.15
Dy_2BTC_3	9.82	14.07	49.81
Eu_2BTC_3	9.75	14.02	63.25
Tb_2BTC_3	9.89	14.12	42.84
Er_2BTC_3	9.85	14.36	43.54

Table 1 Lattice parameters and crystal size

	Ionic Ratio (Å)	Atomic mass (amu)
Nd	1.249	144.24
Eu	1.206	151.96
Gd	1.193	157.30
Tb	1.180	158.93
Dy	1.167	162.50
Er	1.144	167.26

Table 2 Ionic ratios of used lanthanides and of Gd

Figure 2 shows the infrared spectra of the samples obtained with Nd, Dy, Eu, Tb and Er, it is observed that there are vibration bands at very similar wave numbers, which indicates the presence of the same functional groups, which is to be expected since the materials were obtained with the same precursors and with the same methodology. Additionally, they present the same crystalline structure, as described in the diffractograms obtained.

According to table 3, it can be said that these structures are made up of an aromatic ring (1600, 1475, 880, 850-800, 780, 770-730, 715-685 cm^{-1}), there is the presence of the carboxylate anion that gives rise to two bands: a strong band of asymmetric stretching near 1650-1550 cm^{-1} and a weaker symmetrical stretching band, the band is near 1400 cm^{-1}, it has structures where there are double bonds (1640-1610, 990, 970, 910, 890, 815, 700 cm^{-1}) and single bonds (1375, 720 cm^{-1}) in the structure. In addition, the broad band between 3200-3500 cm^{-1} corresponding to OH groups, which are attributed to solvent molecules (water or ethanol) present in the pores of the structure, is intensified for Nd and Dy. This result indicates that the coordination of water molecules is not indicative of the increase in the framework parameter observed in XRD, so the change is mostly associated with a 5% error in the measurement, rather than with the amount of solvent in the pores. of the material.

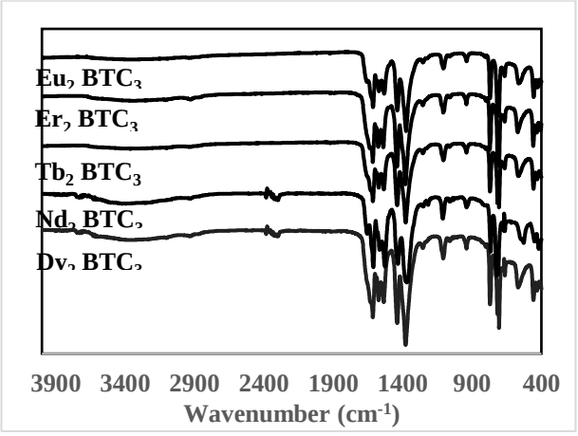

Figure 2 Results obtained by Infrared spectrum by Fourier transform

In addition, it can be said that between 400 and 500 cm^{-1}, there are differences in intensities and this is most probably due to the atomic masses of the elements of the lanthanide series, since, for example, Dy and Er, having greater atomic mass present the most intense peaks see Table 3.

The morphology analysis was achieved only for the Dy_2BTC_3 material at 5,000 and 20,000 magnifications and is presented in Figure 3 (a and b).

ISSN-On line: 2410-4191.

Functional group	Band[a]	Wave number (cm-1)
Aromatics	C=C t	~1600 and ~1475
	C-H d (mono)	770-730 abd 715-685
	C-H d (orto)	770-735
	C-H d (meta)	~880 and ~780 and ~690
	C-H d (para)	850-800
Carboxylate anion	C=O t	1650-1550
	C-O t	1400
t= tension vibration d= deformation		

Table 3 Vibrational modes and functional group band assignments in the FT-IR spectrum
Source: [Domínguez et. to the. 2019]

Homogeneous cubic-shaped crystals with sizes ranging from 100 to 300 nm are observed, however these crystals are made up of particles with sizes ranging from 24-63 nm according to the DRX results. After carrying out the bibliographic review, no reports of micrographs with these shapes or sizes were found for MOFs synthesized with lanthanides, generally the morphology is in micrometer-sized fibers form or rods [Lian & Yan, 2016; Chen, et al., 2022]. This result indicates that the material can be used in nanotechnology in particular as a drug carrier or cell tracer, due to its nanometric size.

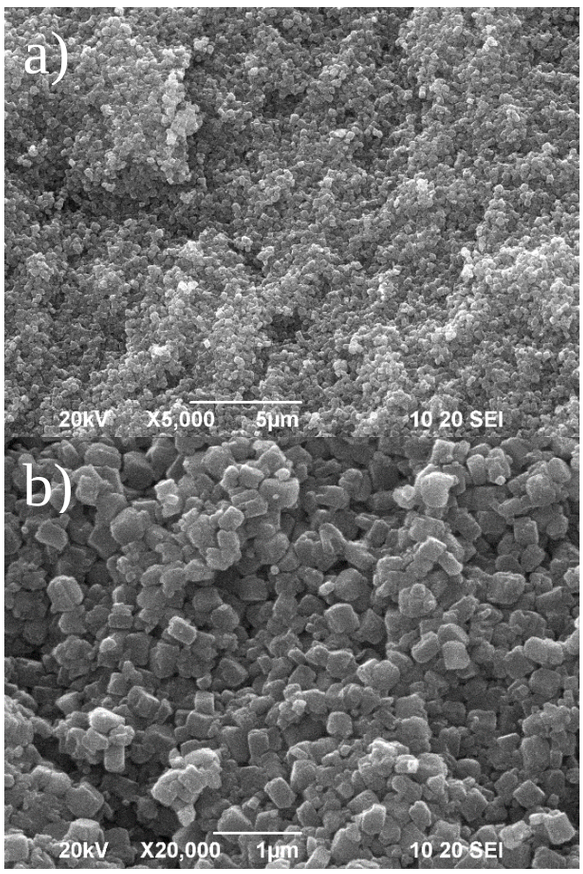

Figure 3 Microscopies of Dy_2BTC_3 at 5,000 magnification (a) and 20,000 magnification (b)

Optical properties of MOFs

The optical properties of the MOFs were obtained only for the luminescent materials (Eu_2BTC_3, Dy_2BTC_3 and Tb_2BTC_3), since Er_2BTC_3 did not present luminescence in the visible region. Figure 4 presents a photo of the materials irradiated with a UV lamp to demonstrate the luminescent property and we observe that the Eu_2BTC_3 MOF has a red color, in the case of Tb_2BTC_3 a green color was present and in the Dy_2BTC_3 MOF it was observed a color between yellow and orange. The emission and excitation spectra of these MOFs were obtained, the results are presented in Figure 5 (excitation spectra), in Eu_2BTC_3 the best excitation energy occurs between 250-260 nm and for Tb_2BTC_3 between 290-300 nm, being the best at 300 nm. approximately and for Dy_2BTC_3 the best excitation energy between 250-260 nm. Once the best excitation wavelength was confirmed, the emission and absorption spectra were obtained. Figure 6 shows the emission spectra, in the case of Eu_2BTC_3 emission bands are observed at 590 nm corresponding to the electronic transition $^5D_0 => ^7F_1$, at 620 nm corresponding to the electronic transition $^5D_0 => ^7F_2$, at 650 nm corresponding to the electronic transition $^5D_0 => ^7F_3$ and 700 nm corresponding to the electronic transition $^5D_0 => ^7F_4$. In the case of the MOF of Tb_2BTC_3 it has emission bands at 480 nm which corresponds to the $^5D_4 => ^7F_6$ transition, at 550 nm due to the $^5D_4 => ^7F_5$ transition, at 580 nm it represents the $^5D_4 => ^7F_4$ electronic transition and at 625 nm due to the transition $^5D_4 => ^7F_3$ [G. Alarcon-Flores et. to the. 2015]. Finally, Dy_2BTC_3 has emission bands at 480 nm corresponding to the $^4F_{9/2} => ^6H_{15/2}$ transition, at 545 nm located at the $^4I_{15/2} => ^6H_{13/2}$ transition, 575 nm corresponding to the $^4F_{9/2}$ transition $=> ^6H_{15/2}$ and 620 nm that is observed in the transition $^4I_{15/2} => ^6H_{11/2}$. [Bunzli & Eliseeva (2010)]

Figure 4 Eu_2BTC_3, Dy_2BTC_3, Er_2BTC_3 and Tb_2BTC_3 MOFs.

ISSN-On line: 2410-4191.

Figure 7 presents the excitation and absorption spectra of Eu_2BTC_3, Dy_2BTC_3 and Tb_2BTC_3. It is observed that the bands for the spectra begin to decay the absorption band between 300 nm and 350 nm. In the Eu_2BTC_3 MOF from 250 nm to 310 nm, excitation and absorption are very similar, so it can be said that where it absorbs more energy, the emission intensity will also be much higher, after 310 nm there is a great difference in intensity and it is said that this MOF will absorb much more energy, but the emission intensity will be much lower.

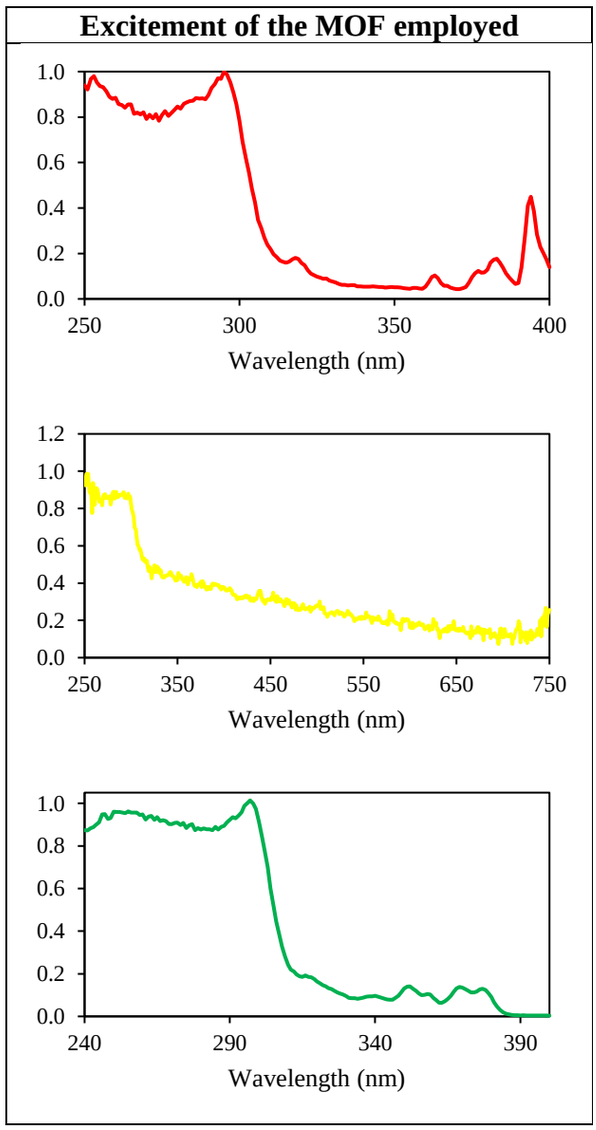

Figure 5 Excitation spectra of Eu_2BTC_3 (red), Dy_2BTC_3 (yellow) and Tb_2BTC_3 (green)

In the case of the MOF of Tb_2BTC_3 it can be seen that it is the same excitation and absorption energy and this excitation energy will produce the maximum intensity. Finally, in the MOF of Dy_2BTC_3 in most of the excitation spectrum it is of lower intensity than the absorption intensity, so it is said that the energy that it absorbs will be greater than the one that is going to be used to emit.

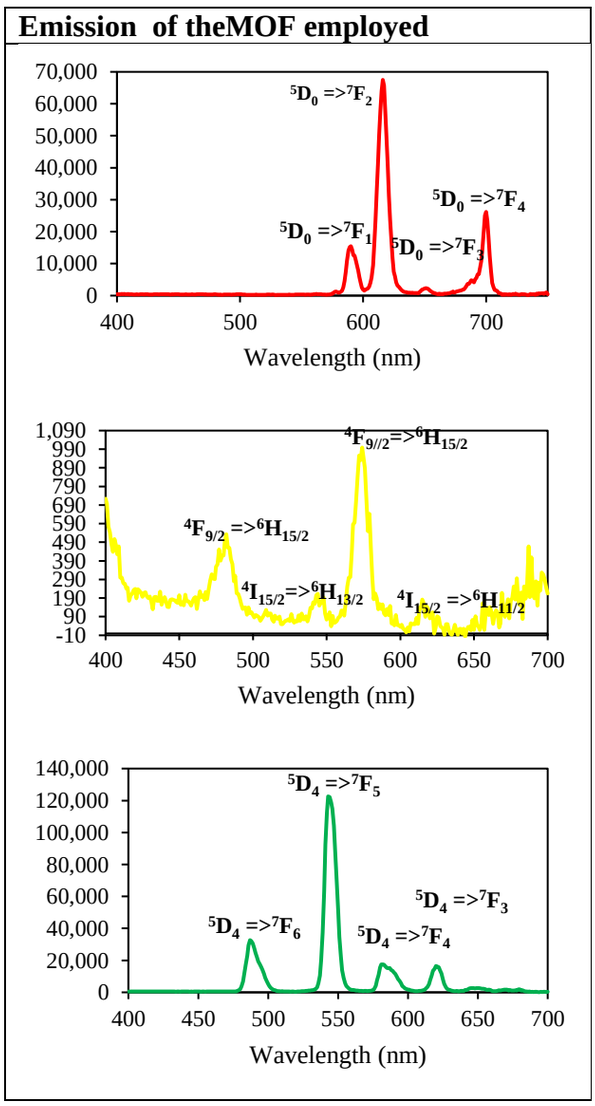

Figure 6 Emission spectra of Eu_2BTC_3 (red), Dy_2BTC_3 (yellow) and Tb_2BTC_3 (green)

ISSN-On line: 2410-4191.

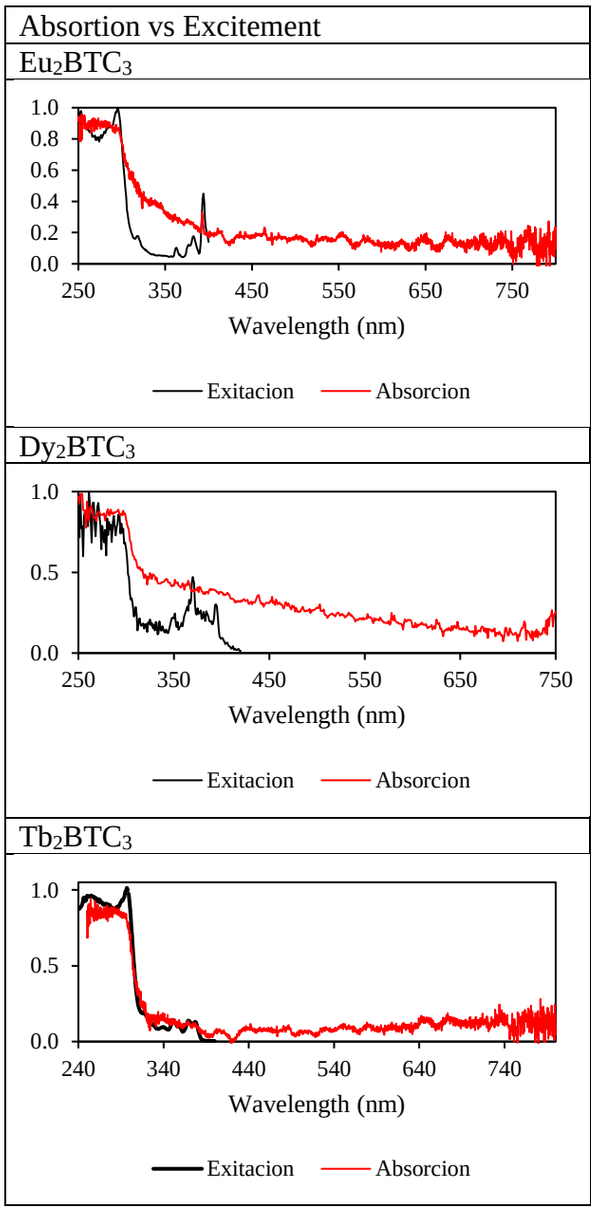

Figure 7. Excitation vs absorption of the synthesized samples

Acknowledgment

To Universidad Autónoma Metropolitana, Azcapotzalco Unit and IPN-CICATA- Legaria Unit for the facilities to carry out this work.

Financing

Funding: This work has been funded by CONAHCYT [grant number 31624, project CB A-S1-31186].

Conclusions

Using the metathesis methodology proposed in this work, which consists of a double displacement chemical reaction, it was possible to obtain five lanthanide metal-organic frameworks at room temperature. The structures obtained are isoreticular with the MOF Gd-BTC, however the synthesis did not require high temperatures, an acid environment or carcinogenic solvents such as DMF. MOFs are nanometric crystals in size and the crystallinity of the structure varies depending on the metallic center used, which changes in ionic radius, electronegativity and solubility, determining parameters in this type of synthesis. In the FT-IR spectra there are vibration bands associated with characteristic functional groups of the 3D framework, with little presence of solvent, it is also highlighted that the band between 400 and 500 cm^{-1} presents a difference in intensity, due to the difference between the atomic weights of the different elements of the lanthanide series, in addition the band between 3200 and 3500 cm^{-1} corresponding to -OH groups, indicates the coordination of water molecules or ethanol molecules present in the pores of the structure, observing that it intensifies for the elements Nd and Dy. The LnMOF presented the antenna effect, which implies that the material takes advantage of the greater amount of energy that is absorbed to produce the emission. This antenna effect occurred when the organic binder absorbed the energy radiated to it, later the absorbed energy was transferred to the lanthanide, which is responsible for carrying out the emission in the visible region of the electromagnetic spectrum. In the absorption and excitation tests, it was found that all the synthesized MOFs present the same absorption spectrum as the BTC structure and by comparing the excitation spectra with the absorption spectra it was determined that there are more wavelengths where energy can be absorbed. to be able to broadcast. The MOFs that presented luminescence were those of Eu, Tb and Dy, being the most intense that of terbium. The results indicate that it is possible to use these materials in nanotechnology applications, so the decrease in the amount of precursors used and the low toxicity is of great importance for the synthesis of MOFs.

ISSN-On line: 2410-4191.

References

Cárdenas Saavedra, J. C. (2019). Tesis de Doctorado. Síntesis, caracterización y evaluación de redes metalo-orgánicas (MOFs) como posibles sensores de metano. Universidad Nacional de Colombia, *Departamento de Química*.

Chen, Z., Lin, X., Liang, J., Wang, C., Min, J., Wang, Y., & Huang, Y. (2022). Synthesis ofGd (III)-MOF: Dy3+ phosphor and kinetics study of its thermal decomposition. Journal ofThermal Analysis and Calorimetry, 147(12), 6817-6823. DOI: https://doi.org/10.1007/s10973-021-11003-x

Domínguez-Pérez, L. A., Lagunes-Gálvez, L. M., Barajas-Fernández, J., Olán-Acosta, M. D. L. Á., García-Alamilla, R., & García-Alamilla, P. (2019). Caracterización vibracional de grupos funcionales en granos de cacao durante el tostado usando espectroscopía de infrarrojo por transformada de Fourier. *Acta universitaria*, *29*. DOI: https://doi.org/10.15174/au.2019.2172.

Farha, O. K., Eryazici, I., Jeong, N. C., Hauser, B. G., Wilmer, C. E., Sarjeant, A. A., Snurr R. Q., Nguyen S. T., Yazaydın A. Ö., & Hupp, J. T. (2012). Metal–organic framework materials with ultrahigh surface areas: is the sky the limit?. *Journal of the American Chemical Society*, 134(36), 15016-15021. DOI: https://doi.org/10.1021/ja3055639

Alarcón-Flores, G., García-Hipólito, M., Aguilar-Frutis, M., Carmona-Téllez S., Martínez-Martínez, R., Campos-Arias, M.P., Zaleta-Alejandre, R., & Falcony, C. (2015). Synthesis and fabrication of Y_2O_3:Tb^{3+} and Y_2O_3:Eu^{3+} thin films with electroluminescent applications: Optical and structural characteristics. Materials Chemistry and Physics vol 149-150, 34-42 (2015). DOI: https://doi.org/10.1016/j.matchemphys.2014.09.020

Garduño-Wilches, I. A., Alarcón-Flores, G., Carro-Gastélum, A., Carmona-Téllez, S., Aguilar-Frutis, M. A., & Loera-Serna, S. (2021). Enhanced photoluminescence quantum yield of terbium nano-MOFs synthesized by microwave assisted solvothermal method. *Nano-Structures & Nano-Objects*, *26*, 100736. DOI: https://doi.org/10.1016/j.nanoso.2021.100736

Bunzli, J. C. G, & Eliseeva, S. V. (2010) Basics of Lanthanide Photophysics chapter In book: Springer Series on Fluorescence. Lanthanide Luminescence: Photophysical, Analytical and Biological Aspects Edition: 1Publisher: Springer Verlag

Lian, X., & Yan, B. (2016). A lanthanide metal–organic framework (MOF-76) for adsorbing dyes and fluorescence detecting aromatic pollutants. *RSC advances*, 6(14), 11570-11576. DOI: https://doi.org/10.1039/C5RA23681A.

Medina-Velazquez D. Y., Alejandre-Zuniga B. Y., Loera-Serna S., Ortiz E. M., Morales-Ramirez A. D. J., Garfias-Garcia E., Garcia-Murillo A. & Falcony C. (2016). An alkaline one-pot reaction to synthesize luminescent Eu-BTC MOF nanorods, highly pure and water-insoluble, under room conditions. Journal of Nanoparticle Research, 18, 1-10. DOI: https://doi.org/10.1007/s11051 016-3593-9.

Pérez Carrasco, C., Medina Velázquez, D. Y., Garfias García, E., Colín Luna, J. A., Barrón Meza, M. Á., & Reyes Miranda, J. (2020). Análisis estructural y luminiscente de redes metal orgánicas de tenoltrifluoroacetona tridopadas con tierras raras. https://revistatediq. azc. uam. mx/Docs/Revista_TeDIQ_2020. pdf.

Porcher, P., Puche, R. S., Maestro, P., & Cascales, C. (2000). Tierras raras: materiales avanzados. In Anales de la Real Sociedad española de Química (No. 4, pp. 11-26). Real Sociedad Española de Química. ISSN-e 2792-5250.

Ríos Carvajal, T. (2014). Síntesis y caracterización de redes metal-orgánicas (MOF) a partir de ligantes orgánicos tipo fenilenvinileno modificados con grupos electrodonores. Departamento de Química. https://repositorio. unal.edu.co/handle/unal/52813

Rocío-Bautista, P. (2019). Redes metal-orgánicas como alternativa. BOLETÍN GRASEOA, 3. https://analesdequimica.es/ index.php/AnalesQuimica/article/view/1515

Sánchez, R. M. Determinación de lantánidos mediante espectroscopía de descomposición inducida por láser. https://core.ac.uk/download/ pdf/289986509.pdf

ISSN-On line: 2410-4191.

Wang, H., Zhao, D., Cui, Y., Yang, Y., & Qian, G. (2017). A Eu/Tb-mixed MOF for luminescent high-temperature sensing. Journal of Solid State Chemistry, 246, 341-345. DOI:10.1016/j.jssc. 2016.12.003.

ISSN-On line: 2410-4191.

Article **ECORFAN Journal-Bolivia**
June 2023, Vol.10 No.18 10-15

Development and physicochemical evaluation of a snail protein-based worcestershire sauce (*Helix aspersa*)

Desarrollo y evaluación fisicoquímica de una salsa inglesa con proteína de caracol (*Helix aspersa*)

REYNOSO-OCAMPO, Carlos Abraham†*, ARROYO-CRUZ, Celerino and TREJO-TREJO, Elia

Universidad Tecnológica del Valle del Mezquital, Hgo., Mexico.

ID 1st Author: *Carlos Abraham, Reynoso-Ocampo* / **ORC ID:** 0000-0002-1620-584X, **Researcher ID Thomson:** T-2543-2018, **CVU CONAHCYT ID:** 9631

ID 1st Co-author: *Celerino, Arroyo-Cruz* / **ORC ID:** 0000-0002-7027-101, **Researcher ID Thomson:** T-2543-2018, **CVU CONAHCYT ID**: 7382

ID 2nd Co-author: *Elia, Trejo-Trejo* / **ORC ID:** 0000-0003-0184-1795, **Researcher ID Thomson:** ISB-6748-2023, **CVU CONAHCYT ID:** 419229

DOI: 10.35429/EJB.2023.18.10.10.15 Received: January 15, 2023; Accepted: June 30, 2023

Abstract

The garden snail, *Helix aspersa*, is a common species and its flesh is rich in high biological value proteins that provide all the essential amino acids for nutrition. Based on this, the aim of this study was to utilize snail protein in the development of an English-style sauce to add value. The formulation was developed and the physicochemical and microbiological characteristics of the resulting product were evaluated, ensuring the quality and safety of the process. The obtained results indicated that, once the English-style sauce with snail protein was standardized, the physicochemical parameters of pH, ºBx, and acidity did not show significant differences compared to the control sauce. This suggests that consumers accustomed to consuming commercial English-style sauce will not perceive differences when trying the sauce made with garden snail. In conclusion, the development of an English-style sauce with snail protein has the potential to add value to the product, taking advantage of the high protein quality of the garden snail. This may be of interest to the food industry in product diversification and the promotion of unconventional food consumption.

***Helix*, Physicochemical parameters, microbiological evaluation**

Resumen

El caracol de jardín, *Helix aspersa*, es una especie común y su carne es rica en proteínas de alto valor biológico, que aportan todos los aminoácidos esenciales para la alimentación. Con base en esto, el presente estudio tuvo como objetivo aprovechar la proteína de caracol en el desarrollo de una salsa tipo inglesa para agregarle valor. Se desarrolló la formulación y se evaluaron las características fisicoquímicas y microbiológicas del producto obtenido, con lo que se aseguró la calidad e inocuidad del proceso. Los resultados obtenidos indicaron que, una vez que la salsa tipo inglesa con proteína de caracol fue estandarizada, los parámetros fisicoquímicos de pH, ºBx y acidez no mostraron diferencias significativas en comparación con la salsa control o testigo (SIC). Esto sugiere que los consumidores habituados al consumo de salsa inglesa comercial no percibirán diferencias al probar la salsa elaborada con caracol de jardín. En conclusión, el desarrollo de una salsa tipo inglesa con proteína de caracol presenta un potencial para añadir un valor agregado al producto, aprovechando la alta calidad proteica del caracol de jardín, lo que puede ser de interés en la industria alimentaria en la diversificación de productos y la promoción del consumo de alimentos poco convencionales.

***Helix*, Parámetros fisicoquímicos, evaluación microbiológica**

Citation: REYNOSO-OCAMPO, Carlos Abraham, ARROYO-CRUZ, Celerino and TREJO-TREJO, Elia. Development and physicochemical evaluation of a snail protein-based worcestershire sauce (*Helix aspersa*). ECORFAN Journal-Bolivia. 2023. 10-18:10-15.

* Correspondence to Author (E-mail: aestrada@itesa.edu.mx)
† Researcher contributing as first author.

Introduction

The worldwide consumption of land snails is widespread in the world, particularly in Europe, where France is the main consumer of snails in the world. Within the denomination of snails are included a great diversity of species that present some very evident morphological differences. The most common snail, known as garden snail or common land snail is the species *Helix aspersa*. Other species are the Roman snail (*Helix pomatia*), the Turkish snail (*Helix lucorum*) and the Christian snail (*Otala punctata*). This mollusk is considered a delicacy and is a must in most famous restaurants. There are several ways of commercialization for the land snail, among which are: live, frozen, and packaged. The main producing countries are located in the northern hemisphere in areas close to France, with Greece and Turkey standing out as the main suppliers of the French market.

In this research it is assumed that the garden snail is a valuable food resource due to its nutritional properties and potential in the food industry. While its production and processing can be difficult, there has been promising research on its use in processed food production and as an ingredient in food production (Krzeminska, *et al*, 2017; Cofrades, *et al*, 2016). Due to the above and with the aim of contributing to the food industry, the present research has been developed, whose objective is to formulate an innovative Worcestershire sauce that incorporates snail protein (*Helix aspersa*) as a functional ingredient, in order to improve the nutritional value of the final product and contribute to the sustainable use of the snail as a raw material. This is justified given that more research is needed to explore the potential of snails in the food industry.

On insects in the development of new products

In recent decades, food production has been the subject of increasing concern regarding its sustainability. The search for alternative protein sources to meat has led to the exploration of new sources, such as edible insects. According to FAO, insects are a food source rich in protein, vitamins and minerals, and are more sustainable than traditional protein sources due to their low environmental impact (García-Gómez *et al*., 2020).

Within the animal group, minor species that have potential, such as mollusks that have potential, such as mollusks and insects have been used for centuries in human food in various parts of the world, however, only recently have their nutritional properties and their potential in the food industry been further investigated (Rumpold and Schlüter, 2013). Insects are rich in protein, healthy fats, vitamins and minerals, and many of them contain a significant amount of essential fatty acids and amino acids that our body cannot synthesize Garcia (idem). In addition, insects have a lower environmental impact than traditional farm animals, as they require less land, water and feed to produce the same amount of protein (Van Huis *et al*., 2013). Despite the nutritional benefits of insects, there is still some cultural rejection of their consumption; the development of new innovative and attractive food products for consumers could help overcome this barrier and take advantage of their nutritional benefits.

About the garden snail (Helix aspersa)

The garden snail (*Helix aspersa*) is a species of gastropod commonly used in food processing, such as French cuisine. This snail is prized in many places for its edible meat and is therefore considered an important food resource. In addition to its gastronomic value, the garden snail is also valued for its nutritional properties and its potential in the food industry has been investigated (Adegoke, *et al*.,2016).

Krzeminska (ibidem) asserts that the garden snail is a good source of protein and essential fatty acids, such as linoleic acid and oleic acid. In addition, it contains a wide variety of vitamins and minerals, such as iron, zinc, selenium and vitamin B12. However, its use in the food industry is limited due to the difficulty of its production and processing. Despite this, studies have been conducted on the use of snail in the production of processed foods, such as hamburgers and sausages, with promising results as mentioned by Krzeminska (ibidem). In addition, the use of snail meal in food production has also been investigated. A study by Cofrades (ibidem) found that the addition of snail flour to empanada dough improved its nutritional and sensory value, with a higher amount of protein and minerals. On the other hand, Montowska *et al*. (2018) found that garden snail meat has a high nutritional quality, similar to that of chicken meat.

ISSN-On line: 2410-4191

The above research, shows the potential of the snail to be used as another ingredient in the development of new food products, such as the one that concerns us in this research.

About Worcestershire sauce

Worcestershire sauce, commonly called Worcestershire, is a popular and widely used condiment in international cuisine. Its distinctive umami flavor and culinary versatility have led to an increasing demand and exploration of new formulations and improvements in its composition (Jones *et al*., 2021).

In analyzing recent research, several trends and advances in the formulation and application of Worcestershire sauce were found. A study conducted by Montowska (ibidem) focused on the reduction of sodium content; while Jones (ibidem) explored the use of natural and fermented ingredients in the production of Worcestershire sauce, with the aim of improving its nutritional profile and increasing its added value. Lee *et al*., (2023) focused on the development of Worcestershire sauces with specific flavors, such as citrus or smoked notes, using natural extracts and flavoring techniques. These findings support the importance of continued research and innovation in the condiment industry in order to meet changing consumer demands and promote healthier culinary choices, as a Worcestershire sauce with hydrolyzed Helix aspersa protein results.

Materials and methods

Experimental research was carried out for the development of a new product in which a main ingredient is the addition of snail in order to add more nutritional value to the product. Consequently, the research was developed in the following stages.

Collection and preparation of the snail (*Helix aspersa*): The snail used in the preparation of the Worcestershire sauce was collected during the months of September-October in plots in the municipality of Ixmiquilpan Hidalgo. Once the snails were in the UTVM laboratories, they were dehydrated. With a solution of 75% water at a temperature of 23º C and 25% calcium hydroxide, leaving it to stand for 24 hours, so that the snail would expel the fecal feces and eliminate the mucus or slime of the snail.

Then the snail meat was washed with purified water to remove impurities. The soybeans were then cooked in a kettle at 95-97°C for one hour, and then homogenized and mixed (50% snail and 50% soy) for 30 minutes. A dough was obtained, which was laminated until obtaining a thickness of 1.5 cm, to be later sectioned into 2 X 2 cm cubes. The sectioned cubes were left to rest in an incubator for 8 days at a temperature of 36° C. After incubation, a 2% brine was prepared, introducing the cubes until they were completely covered. It was left to ferment for 30 days at a temperature of 25°C and with intermittent mixing every day at 15-20 rpm. for 5 minutes. This first stage is concluded by filtering the insoluble solids, recovering the miscible liquid for the final mixture.

Formulation and standardization of the production process:

Worcestershire sauce was made by adding traditional ingredients, to the liquid recovered in the previous stage, in the following proportions: Pepper (0.5%), Onion (0.1%), Garlic (0.28%), Salt (0.5%), Ginger (0.28%), Mustard (0.1%), Cinnamon (0.64%), Sugar (0.3%), 5% acetic acid was added to hydrolyze the miscible liquid to incorporate the soy protein and mainly snail protein into the sauce. Subsequently, it was filtered to separate the larger particles and thus obtain a liquid free of sediment. The sauce was pasteurized for 30 minutes at 75ºC, and potassium sorbate (0.1%) and sodium benzoate (0.1%) were added as preservatives. Finally, the product was packaged at a temperature of 85º C to generate vacuum in an amber-colored container.

Physical-chemical analysis:

Physicochemical analyses were performed on the final product according to the methods recommended by the Association of Official and Analytical Chemists (AOAC, 1984). These included the determination of acidity, pH, carbohydrate content, fat, protein, moisture and minerals. The results obtained were expressed as mean ± standard deviation. The results obtained were compared with those of a commercial Worcestershire sauce (SIC), the intention of which was to match the flavor and/or mask the flavor of the snail so that the consumer would not detect the differences in flavor, odor and texture of the new product.

ISSN-On line: 2410-4191

To determine the differences between the Worcestershire sauce with Helix (SIH) and the SCI, the results were analyzed with a randomized block design with a significance level of α=0.5, with six replications; the SCI was considered as a control, for which a Dunnet's test of contrasts was performed with α=0.5. Minitab ver 21.1 was used for statistical analysis.

Microbiological analysis:

Microbiological analyses were performed according to the Mexican Official Standard NOM-130-SSA1-1995.Tests were carried out for the detection and enumeration of pathogenic microorganisms, such as coliform bacteria, Salmonella spp. and Staphylococcus aureus, as well as mesophilic aerobic counts and fungi and yeasts. Seeding techniques were followed in appropriate culture media and viable counts were performed for each target microorganism.

Shelf-life evaluation:

A shelf life study was conducted to determine the stability of the developed sauce. The stability of the sauce was evaluated at 30, 60 and 90 days keeping the temperature under control (25ºC) pH. These were the response variables to evaluate changes in the quality of the product over time. Periodic measurements were taken and statistically analyzed to determine the evolution of the variables as a function of time and storage temperature.

Results and discussion

Standardization of the production process

To obtain the final formulation of Worcestershire sauce with snail (*Helix aspersa*), it was necessary to make different formulations until achieving one that would match the sensory characteristics of commercial Worcestershire sauce (SIC). Table 1 shows this formulation; the use of the garden snail, which increased the protein value of the product, stands out.

Ingredient	Quantity (%)
Snail meat	50
Wheat flour	68
Apple vinegar	4
Apple juice	3
Pepper	0.5
Onion	0.1
Garlic	0.28
Salt	2
Ginger	0.28
Mustard	0.1
Cinnamon	0.64
Water	0.3

Table 1 Formulation of Worcestershire sauce with *Helix aspersa.*
Source: Own elaboration (2022).

Once the formulation was similar to the SIC, the process was standardized, which is described below (Figure 1). It is important to detail that during the process it was observed that the control points that directly impact the quality of the final product were fermentation and hydrolysis due to the separation of the amino acids that make up the mollusk protein.

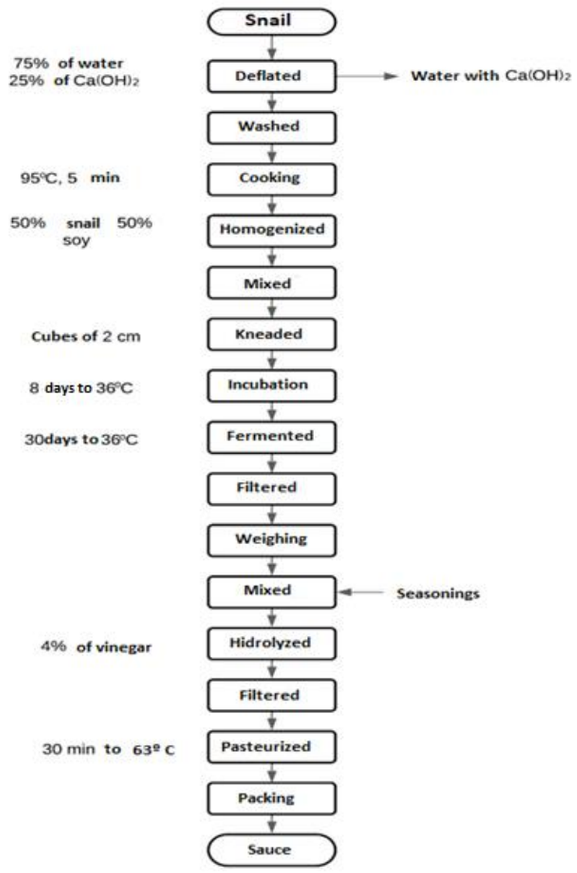

Figure 1 Standardization of the process of elaboration of Worcestershire sauce with *Helix aspersa.*
Source: Own elaboration, (2022).

ISSN-On line: 2410-4191

Physicochemical analysis

Once the SIH was standardized, its pH, ºBx and acidity expressed in percentage of acetic acid were evaluated (Table 2). It was found that these parameters did not show a significant difference in relation to the control or control treatment (SIC) with an α=0.05. This suggests that the consumer who is accustomed to the consumption of commercial Worcestershire sauce will not find a difference with the sauce made with garden snail. This is important because Van Huis et al. (2013) asserts that despite knowing the benefits of consuming some terrestrial insects and mollusks, the population is reluctant to consume them and even to try them.

Parameter	SIH	SIC
pH	3.5±0.183[a]	3.6±0.152[a]
ºBx	10.3±0.130[a]	10.2±0.113[a]
Acidity (% of acetic acid)	4.11±0.121[a]	4.15±0.118[a]
Note: Different letters, for each parameter evaluated, indicate significant difference (p<0.05).		

Table 2 Comparative evaluation of physicochemical parameters of Worcestershire sauce with *Helix aspersa* vs. commercial Worcestershire sauce.
Source: Own elaboration, (2022).

According to the results of the proximate chemical analysis presented in Table 3, it can be observed that the developed sauce presents a higher content of moisture, fat, protein and minerals, with percentages of 91.5%, 0.8%, 1.0% and 1.5%, respectively. These differences are statistically significant (α=0.5) compared to the control (SIC). This is explained by the fact that the elaborated sauce presents an increase in protein content of 243.9 % with respect to the control sample. It is important to note that the commercial sauce shows a higher carbohydrate content, mainly because it contains elements rich in carbohydrates such as molasses and corn syrup, and in some cases piloncillo.

Parameter	SIH (100g)	SIC (100g)
Moisture (%)	91.5±1.109[a]	82.09±0.987[b]
Fat (%)	0.8±0.012[a]	0.2±0.009[b]
Protein (%)	1.0±0.123[a]	0.41±0.087[b]
Carbohydrate (%)	5.2±0.143[a]	16.1±1.89[b]
Minerals (%)	1.5±0.120[a]	1.2±0.113[a]
Note: Different letters, for each parameter evaluated, indicate significant difference (p<0.05).		

Table 3 Proximal chemical analysis of Worcestershire sauce with *Helix aspersa* vs. commercial Worcestershire sauce.
Source: Own elaboration, (2022).

Microbiological analysis

After performing the microbiological analyses corresponding to the sauce developed, it was found that all the parameters established in NOM-130-SSA1-1995 are within the maximum limits allowed by current regulations (Table 6). This means that the garden snail Worcestershire sauce complies with the quality and safety standards required for its commercialization and consumption.

Determination	SIH	Maximum Permissible Limits (CFU/g)
Fungi	7	20
Yeasts	20	50
Total and fecal coliforms	0	0

Table 4 Microbiological analysis of Worcestershire sauce with *Helix aspersa* vs. commercial Worcestershire sauce.
Source: own elaboration (2022).

Shelf-life tests (product stability)

Table 5 shows the stability of Worcestershire sauce with snail at different storage times (30, 60 and 90 days) at a controlled temperature of 25ºC. It is observed that the Brix degrees (°Bx) decrease with time, which is explained by the possible fermentation of the sugars present in the sauce, leading to a reduction in sugar content and, therefore, in soluble solids. According to Lee (ibidem) this phenomenon can affect the texture and flavor of the sauce, so it is important to constantly monitor the soluble solids content during storage to ensure that quality standards are met. On the other hand, pH tends to decrease over time due to microbial activity and the production of acetic acid and other organic acids as a result of ingredient fermentation. However, the decrease in pH is observed to be slow due to storage temperature and the specific composition of Worcestershire sauce. However, as suggested by Jones (ibidem), periodic pH monitoring during storage is crucial to ensure product quality and safety.

Days	pH
30	3.217±0.183
60	3.182±0.093
90	3.417±0.141

Table 5 Stability of Worcestershire sauce with *Helix aspersa* at 25ºC.
Source: Own elaboration, (2022).

ISSN-On line: 2410-4191

Conclusions

In conclusion, the results of this research demonstrate that it is technically feasible to develop an English-type sauce using snail protein. The physicochemical analyses performed are within the parameters established for sterilized products with a pH ≤ 4.5, in accordance with NOM-130-SSA1-1995. From the microbiological point of view, it was determined that the product is innocuous, which guarantees its safety for consumption and provides reliability.

One of the main advantages of this development is its high protein content compared to the commercial product, as well as the reduction of carbohydrates since it does not contain added sugars. This can be a positive aspect for consumers seeking healthier and more nutritious food options.

To continue advancing the study, immediate future research involving product acceptance tests with a group of experts is suggested, with the objective of confirming its viability in the market and evaluating its potential for purchase. These evaluations will allow obtaining valuable information on the acceptability and consumer perception of snail sauce, which will be fundamental for its subsequent commercialization and positioning in the sauce market.

References

Association of Official and Analytical Chemists (1984). *Official Methods of Analysis. 14th*. Ed. Arlington.

Cofrades, S., López, L. I., Solas, M. T., Bravo, L., & Jiménez, C. F. (2016). Nutritional and sensory properties of empanadas made with wheat flour and snail meat flour. *Food Science and Technology International*, *22*(5), 421-430. Retrieved August 11, 2023, from: https://doi.org/10.1177/1082013216647669

García-Gómez, B., Varela, P., Sánchez-Muros, M. J., Ramos-Elorduy, J., & Morales-Ramos, J. A. (2020). Insectos comestibles: potencialidades y limitaciones en la alimentación humana. Alimentación. *Nutrición y Salud, 27(3), 53-60.*

Jones, A. B., Johnson, C. D., & Thompson, R. F. (2021). Exploring the use of natural and fermented ingredients in Worcestershire sauce. *Journal of Food Science, 86*(5), 1682-1689.

Lee, S. H., Park, J. W., & Kim, J. Y. (2023). Development of customized flavors in Worcestershire sauce using natural extracts. *Food Chemistry*, 370, 131087.

Krzeminska, M., Dudek, K., Winarski, R., & Zawadzki, W. (2017). Use of snail meat in the production of processed meat products–a review. *Journal of Food Processing and Preservation, 41*(5), e13260. https://doi.org/10.1111/jfpp.13260.

Montowska, M., Pospiech, E., & Babij, K. (2018). Nutritional value and potential health benefits of snail meat: a review. *Journal of the Science of Food and Agriculture, 98*(13), 4793-4800.

Rumpold, B. A., & Schlüter, O. K. (2013). Nutritional composition and safety aspects of edible insects. *Molecular Nutrition & Food Research, 57*(5), 802-823. Retrieved August 11, 2023, from: https://doi.org/10.1002/mnfr.201200735

Van Huis, A., Van Itterbeeck, J., Klunder, H., Mertens, E., Halloran, A., Muir, G., & Vantomme, P. (2013). Edible insects: Future prospects for food and feed security. *FAO Forestry Paper, (171)*, 1-201. Retrieved August 11, 2023, from: https://www.fao.org/3/i3253e/i3253e.pdf.

ISSN-On line: 2410-4191

Article **ECORFAN Journal-Bolivia**
June 2023, Vol.10 No.18 16-23

Chromate resistance in *Cupriavidus metallidurans* CH34: molecular modeling from ChrC superoxide dismutase

Resistencia a cromato en *Cupriavidus metallidurans* CH34: modelamiento tridimensional de la superóxido dismutasa ChrC

DÍAZ-PÉREZ, Alma Laura´†, CASTRO-MORENO, Patricia´´, VELOZ-GARCÍA, Rafael Alejandro´´´ and DÍAZ-PÉREZ, César´´´*

´Instituto de Investigaciones Químico-Biológicas, Universidad Michoacana de San Nicolás de Hidalgo.
´´Unidad de Biomedicina, División de Investigación y Posgrado, Facultad de Estudios Superiores Iztacala, UNAM.
´´´Departamento de Ingeniería Agroindustrial, Campus Celaya-Salvatierra, Universidad de Guanajuato.

ID 1st Author: *Alma Laura, Díaz-Pérez* / **ORC ID:** 0000-0002-6418-5708, **CVU CONACHYT ID:** 92282

ID 1st Co-author: *Patricia, Castro-Moreno* / **ORC ID:** 0000-0002-3211-0728, **CVU CONACHYT ID:** 164454

ID 2nd Co-author: *Rafael Alejandro, Veloz-García* / **ORC ID:** 0000-0002-6493-5708, **CVU CONACHYT ID:** 163099

ID 3rd Co-author: *César, Díaz-Pérez* / **ORC ID:** 0000-0001-7847-1062, **CVU CONACHYT ID:** 101579

DOI: 10.35429/EJB.2023.18.10.16.23 Received: January 20, 2023; Accepted: June 30, 2023

Abstract

Chromate has become an environmental pollutant present in different ecosystems due to its use in industry. Bacteria have evolved to resist stress produced by chromate. Among chromate-resistance mechanisms we can list Reactive Oxygen Species detoxification systems. Cme-SOD (ChrC) protein from *Cupriavidus metallidurans* CH34 is a superoxide dismutase that mitigate oxidative stress caused by chromate. Cme-SOD protein belongs to Fe and Mn-dependent SOD family (pfam02777). The objective of this study was to analyze the three-dimensional structure of the Cme-SOD protein, for which monomer and tetramer models of the enzyme were built. In the monomer model it was observed that Cme-SOD has a characteristic two-domain structure from iron-dependent SOD, additionally, Cme-SOD has an iron-binding site formed by conserved residues H26 and H75 in the N-terminal domain, and D157 and H161 in the domain C-terminal domain. It was show that chromate stress response SODs have a non-conserved residues in the active site (R37, N59, S71, D143 and Y164). These findings suggest the presence of a novel active site in this family of enzymes.

***Cupriavidus metallidurans* CH34, Fe-superoxide Dismutase, Enzyme**

Resumen

El cromato se ha convertido en un contaminante ambiental presenten en distintos ecosistemas. Las bacterias han evolucionado para resistir el estrés producido por este contaminante. Entre estos mecanismos de resistencia se encuentran los sistemas de detoxificación contra las especies reactivas de oxígeno. La proteína Cme-SOD (ChrC) de *Cupriavidus metallidurans* CH34 es una superóxido dismutasa que ayuda a mitigar el estrés oxidativo causado por el cromato. La proteína Cme-SOD pertenece a la familia de SOD dependientes de Fe y Mn (pfam02777). El objetivo de este estudio fue analizar la estructura tridimensional de la proteína Cme-SOD, para lo cual se construyeron modelos del monómero y del tetrámero de la enzima. El modelo del monómero reveló que Cme-SOD presenta la estructura de dos dominios característica de las SOD dependientes de hierro, cuenta con un sitio de unión a hierro formado por los residuos conservados H26 y H75 en el dominio N-terminal, y D157 e H161 en el dominio C-terminal. Se observó que las SOD que responden al estrés por cromato tienen residuos no conservados en el sitio activo (R37, N59, S71, D143 y Y164). Estos hallazgos sugieren la presencia de un sitio activo novedoso en esta familia de enzimas.

***Cupriavidus metallidurans* CH34, Fe-superóxido-Dismutasa, Enzima**

Citation: DÍAZ-PÉREZ, Alma Laura, CASTRO-MORENO, Patricia, VELOZ-GARCÍA, Rafael Alejandro and DÍAZ-PÉREZ, César. Chromate resistance in *Cupriavidus metallidurans* CH34: molecular modeling from ChrC superoxide dismutase. ECORFAN Journal-Bolivia. 2023. 10-18:16-23.

* Correspondence to Author (E-mail: cesar.diaz@ugto.mx)
† Researcher contributing as first author.

Introduction

Heavy metals (HMs) are those metals with a density greater than 5 g/cm3 (Nies, 1999), among which arsenic, lead, mercury, chromium, cadmium, nickel, selenium and zinc can be named (Duffus, 2002). Some PMs, such as zinc, nickel and copper, are important as trace elements at low concentrations in organisms, however, at high concentrations PMs are toxic, as they produce reactive oxygen species (ROS), alter DNA, disrupt cellular functions and form toxic organic compounds (Nanda *et al*., 2019; Nies, 1999; Ramírez-Díaz *et al*., 2008).

Chromium is a PM that is widely used in industry for electroplating, tanning, in metallurgy, in welding, in the production of pigments and agricultural fertilisers, and in the manufacture of ammunition, so it has now become an environmental pollutant (*Alvarez et al*., 2021). Bacteria have developed several mechanisms to cope with the stress produced by toxic forms of chromium, such as chromate; among these strategies are expulsion by ChrA chromate transport (Aguilar *et al*., 2008; Nies, 2003; Ramírez-Díaz *et al*., 2008), specific and non-specific reduction (Baldiris *et al*., 2018; Mala *et al*., 2020) and the expression of protective systems against ROS (Branco & Morais, 2016; Miranda *et al*., 2005).

Cupriavidus metallidurans CH34, originally named Alcaligenes eutrophus and later *Ralstonia metallidurans* CH34, is a Gram-negative, bacillary bacterium isolated in 1976 (Houba, 1976). Plasmids pMOL28 and pMOL30 were isolated from *C. metallidurans* CH34, which contain genes conferring resistance to zinc, cadmium, cobalt, mercury, arsenic, lead, silver, copper and chromate (Mergeay & Van Houdt, 2021). Chromate resistance was found to be determined by the chrIBACEF genes found in the pMOL28 plasmid, which encode for the proteins ChrI, ChrA, ChrB, ChrC, ChrE and ChrF (Table 1). Of these proteins, the chromate transporter ChrA is the best studied and is indispensable for chromate resistance (Monsieurs *et al*., 2015).

Among the protection systems against reactive oxygen species are the superoxide dismutase (SOD) proteins. SODs are metalloenzymes that catalyse the dismutation of the superoxide anion O^{2-} into oxygen and hydrogen peroxide and are the first line of defence against ROS (Zhao *et al*., 2021). In the chromate protection system of C. metallidurans CH34 are the SODs ChrC and ChrF. Although ChrF has not been functionally characterised, it has 76% sequence identity to the Mn-SOD, ChrF, from *Ochrobactrum tritici* 5bvl1 (Branco & Morais, 2016). SOD ChrC (Cme-SOD) has been biochemically characterised, it is a 197-residue, Fe-SOD-functional protein with a molecular mass of 24 KDa as a monomer; by analytical ultracentrifugation its active form was determined to have a molecular mass of 98 KDa, which means that the functional protein is a tetramer (Juhnke *et al*., 2002). None of these proteins have been structurally characterised by crystallography, nuclear magnetic resonance or electron cryomicroscopy.

Protein	Funtion
ChrI	Transcriptional activator-like protein
ChrA	Transmembrane chromate transporter protein
ChrB	Transcriptional regulator-like protein
ChrC	iron-dependent superoxide dismutase (Fe-SOD)
ChrE	Rhodase-like protein
ChrF	Manganese-dependent SOD-like protein (Mn-SOD)

Table 1 Chromate resistance-related proteins encoded by plasmid pMOL28

Although the SOD ChrC of C. metallidurans CH34 has been experimentally characterised, its three-dimensional structure has not yet been investigated due to the technical difficulties associated with this methodology. One possible solution to obtain its three-dimensional structure is bioinformatics analysis using molecular modelling (Kuhlman & Bradley, 2019). Such a technique has proven to be applicable in numerous cases of SOD (Sánchez-Calderón *et al*., 2019), whose structures have been previously solved and are indispensable to carry out this type of approach accurately. Therefore, the aim of this study is to examine the three-dimensional structure *of C. metallidurans* CH34 Cme-SOD (ChrC) using molecular modelling of the protein, with the purpose of gaining knowledge about its structure and deepening the understanding of the mechanism of action of this enzyme.

ISSN-On line: 2410-4191

Method

Both the monomeric and tetrameric structures of Cme-SOD were modelled. First, a preliminary monomer model was generated using the SWISS-MODEL platform (Waterhouse *et al*., 2018), taking the structure of Clostridium difficile SOD (PDB: 3TJT) as a template. For the construction of the final monomer model, moulds were searched by BlastP (Altschul *et al*., 1997), using the Cme-SOD sequence (Accession number: CAC42412), in the PDB database, with default parameters. Several structures were used as templates; the Fe-SOS from Aquifex pyrophilus (PDB: 1COJ), the Cme-SOD from the AlphaFold database (AlphaFold id: AF-P17550-F1) and the preliminary model generated with SWISS-MODEL. Sequence alignments were carried out in the T-Coffee program (Di Tommaso *et al*., 2011). The final monomer model was generated using Modeller 9v10 (Webb & Sali, 2016). The tetramer model was generated in a similar manner using a primary tetrameric model of the Fe-SOS from *Aquifex pyrophilus* (PDB: 1COJ), a tetrameric overlay of the Cme-SOD from the AlphaFold database (AlphaFold id: AF-P17550-F1) and the previously obtained monomer model as templates. All models were validated using the PROCHECK 3.5 program (Laskowski *et al*., 1993).

The molecular models were visualised and the figures were generated with the PyMOL Molecular Graphics System, Version 2.1.0 (Open-Source), Schrödinger, LLC.

Results and discussion

Obtaining the Cme-SOD model of C. metallidurans CH34

Chromate resistance in the bacterium *C. metallidurans* CH34 is due to a set of proteins that have several functions (Table 1). Among these proteins, the Cme-SOD (ChrC) protein has been characterised, whose three-dimensional structure is not known. To gain a better understanding of the active site of this enzyme, three-dimensional models of the monomer and tetramer of this enzyme were generated using homology modelling.

Although a three-dimensional model of this protein is currently available in the AlphaFold database (Jumper *et al*., 2021), this model does not have its cofactor, an iron ion per subunit, which is vital for the activity of the enzyme, so it was decided to model the protein using a solved structure containing the cofactor. In order to have a better quality model, it was decided to make an initial approximation by generating a model using the SWISS-MODEL system. In this system, the Clostridium difficile Fe-SOD protein (PDB: 3TJT), whose structure was solved with the Fe ion, was used as a template. The generated model contains residues in the areas not physically allowed, so it was decided to generate a better quality model using the Modeller program.

In the search for templates, it was found that the protein of known structure with the highest sequence similarity to Cme-SOD is the Fe-SOS from Aquifex pyrophilus (Apy-SOD, PDB:1COJ). These proteins have 34% sequence identity. This percentage is very low, and is at the limit of what is required to generate a molecular model suitable for structural studies (Khor *et al*., 2015). To generate a high quality model, it was decided to use several structures or models as templates. The casts selected were the monomeric SOD structure of A. pyrophilus, the Cme-SOD model obtained from the AlphaFold database and the model previously generated using SWISS-MODEL. The use of the Apy-SOD and the SWISS-MODEL model allowed us to model the Cme-SOD with the iron ion, and using the Cme-SOD model from AlphaFold does not ensure a high quality mould with 100% coverage of the protein residues. Ten models of the SOD monomer were generated, from which the one with the best structure quality parameters was selected according to the PROCHECK programme that checks the quality of the combinations of the angles φ and ψ on a Ramachandran plot.

The molecular model of the Cme-SOD monomer consists of 197 amino acids, in which a conserved domain characteristic of Mn-, Fe-, Zn- and Cu-dependent SODs (pfam02777) was located. The model presented more than 97% of the residues in the zone of suitable angles and 100% within the zone of allowed angles, and more importantly, none of the angles of the main chain fall within the non-allowed zones (Table 2), which indicates that we have a high quality model (Dalton & Jackson, 2010).

ISSN-On line: 2410-4191

The obtained model was compared by structural alignment with the Apy-SOD structure used as a template, obtaining an RMSD of 0.887 Å. A model with an RMSD deviation of less than 1 Å is indicative of a high-quality model (Dalton & Jackson, 2010). The Cme-SOD monomer shares the characteristics of other Fe-SODs by presenting an architecture with two subdomains, N-terminal and C-terminal. The N-terminal domain consists of α-helices, where part of the active site is located in the first and last helices. The C-terminal domain is formed by three β-strands, surrounded by α-helices, between these helices is the other part of the active site (Figure 1A).

Fe-SODs are conserved proteins found in all three domains of life. It has been reported that in bacteria most Fe-SODs are dimeric, tetrameric Fe-SODs can be found, as is the case for Cme-SOD (Sheng *et al*., 2014). A similar strategy was followed to model the tetramer. The tetramer structure of Apy-SOD, and a tetramer reconstruction of Cme-SOD obtained from the AlphaFold database and the high-quality monomeric model were used as templates. Ten molecular models were reconstructed and verified with PROCHECK, where 100% of the main chain angles were within the allowed angle zone (Table 2). The alignment of the tetrameric model structures yielded an RMSD value of 0.891 Å. These results together do not allow us to conclude that this is a valid model, and of high quality to carry out structural studies. At the interface of the monomers, it can be seen that a loop characteristic of dimeric Fe-SODs is absent, which allows for the correct formation of the tetramer (Sheng *et al*., 2014).

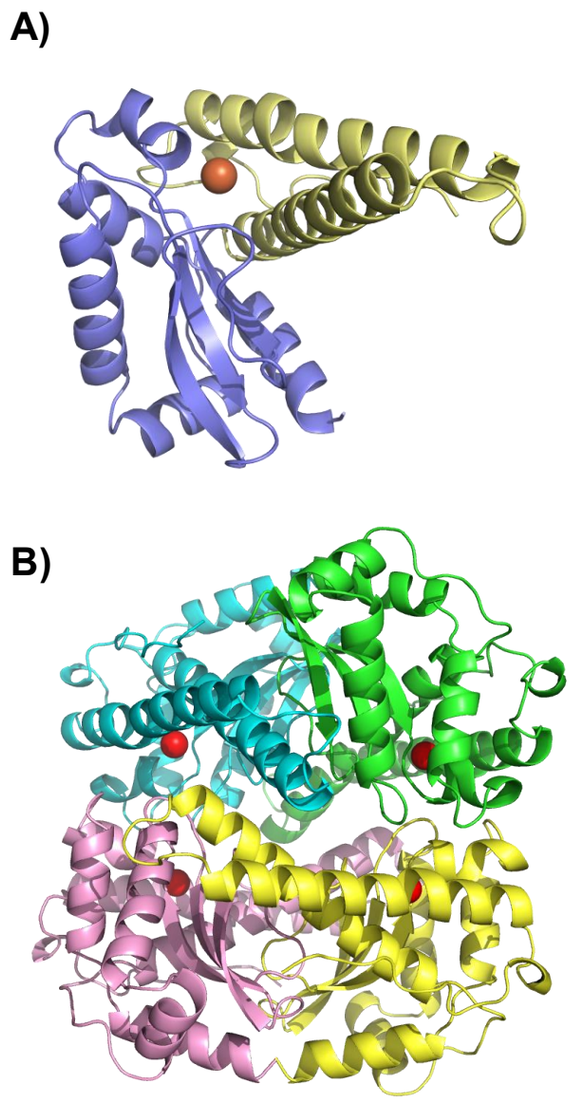

Figure 1 Three-dimensional structure of the Cme-SOD of *C. metallidurans* CH34. A) The structure of the Cme-SOD monomer model is shown. The C-terminal domain is shown in yellow and the C-terminal domain in purple. The iron ion is shown in red. B) The structure of the Cme-SOD tetramer is shown. Each subunit is shown in a different colour. The iron ion of each subunit is shown in red

	Peptide bond angles by region (%)			
Structure	A	P	G	N
1COJ	92.5	7.0	0.5	0.0
Cme-SOD monomer	97.7	2.3	0.0	0.0
Cme-SOD tetramer	97.2	2.8	0.0	0.0

Table 2 Model quality data of the SOD ChrC model of *C. metallidurans* CH34. Ramachandran plot values obtained from the PROCHECK 3.5 program of the molecular model and the Fe-SOD templated protein (1COJ) of A. pyrophilus are shown. A-Adequate. P- Allowed. G-General. N- Not allowed.

ISSN-On line: 2410-4191

Cme-SOD active site analysis of C. metallidurans CH34

Evolutionarily speaking, Fe-SODs were the SODs to appear due to the large amount of iron present and the low oxygen concentration during the emergence of life on earth (Sheng *et al*., 2014). Under modern earth conditions, the retention of iron ion as a cofactor can be explained by the high affinity of the enzyme for iron. The high affinity of Fe-SOD for its cofactor can be explained by a chelating effect of residues in the enzyme active site, in the case of Cme-SOD, the chelating effect is due to four residues with donor groups, in the N-terminal domain H26 and H75, and in the C-terminal domain D157 and H161 (Figure 2). One of the possible advantages of Cme-SOD binding its cofactor by interaction with four residues is its stability despite the entropy generated during the dismutation reaction. The active site is complemented by a water molecule, which connects the four residues that coordinate with the cofactor and gives this region its characteristic trigonal bi-pyramidal geometry (Figure 2).

In the *Escherichia coli* Fe-SOD (PDB:1ISA) it has been observed that residues Y34 and Q69 are part of the active site, being part of the residues that interact with the reaction intermediates (Lah et al., 1995). Comparing the sequence of Cme-SOD with the sequence of 1ISA, it is observed that Q69 of 1ISA has been replaced by S71 in Cme-SOD (Figure 3). However, it is observed that the Y34 position of 1ISA is replaced by A34 in Cme-SOD (Figure 3), which is unable to carry out the interactions necessary for enzyme function, which would undermine the functionality of the enzyme. When analysing the residues in the active site region of Cme-SOD, it is observed that the function of Y34 can be replaced by R37. In Apy-SOD, residues R65, D146 and Y180 have been reported as an important part of the function of this enzyme (Lim et al., 1997), corresponding to residues N59, D143 and Y164 in Cme-SOD, respectively (Figure 3). Both R37, N59 and S71 are conserved in the SOD ChrC protein of O. tritici 5bvl1 and C. metallidurans CH34 and differ in the other Fe-SODs, suggesting that a novel active site has evolved in the chromate stress-responsive Fe-SODs, different from the other Fe-SODs.

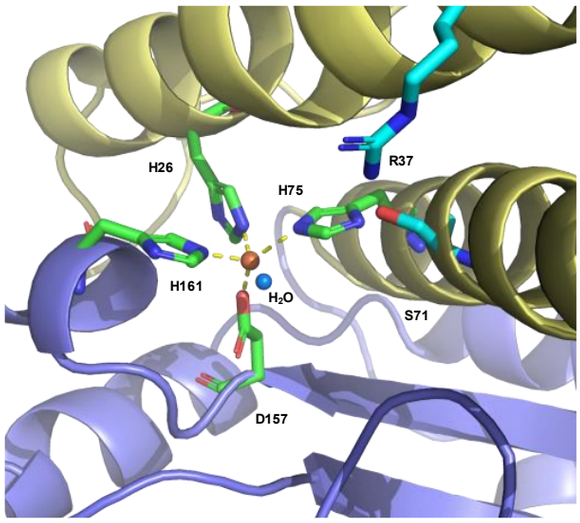

Figure 2 Active site Cme-SOD of *C. metallidurans* CH34. The four conserved residues of the protein that coordinate with cofactor Fe (red) are shown in green. Probable residues complementing the active site are shown in blue. The yellow lines represent the binding between the protein residues and the Fe atom. The complementing water molecule necessary for Cme-SOD function is shown as a blue sphere. Yellow and purple show the amino-terminal and carboxyl-terminal domains respectively

Conclusions

Chromate, a highly toxic form of chromium, induces oxidative stress, damage to organelles, DNA and proteins once it enters cells. There are bacteria that live in environments contaminated with this metal, and these bacteria have developed protective systems against this PM. The ChrC enzyme is one of the enzymes that has been biochemically characterised as an SOD and is present in several chromate-resistant bacteria, such as *P. aeruginosa*, *O. tritici* 5bvl1 and C. metallidurans CH34. The results of this study allow us to conclude that the Cme-SOD protein belongs to a conserved superfamily (pfam02777) with a structure characteristic of iron-dependent SODs and has a conserved iron binding site among the members of this superfamily. In addition, the active site was identified, which is not completely evolutionarily conserved, suggesting that chromate-responsive SOD enzymes possess a novel active site. Knowledge of the structure of Cme-SOD will help us to deepen the understanding of this enzyme family, to better understand the chromate detoxification process and to develop biotechnological tools for bioremediation.

ISSN-On line: 2410-4191

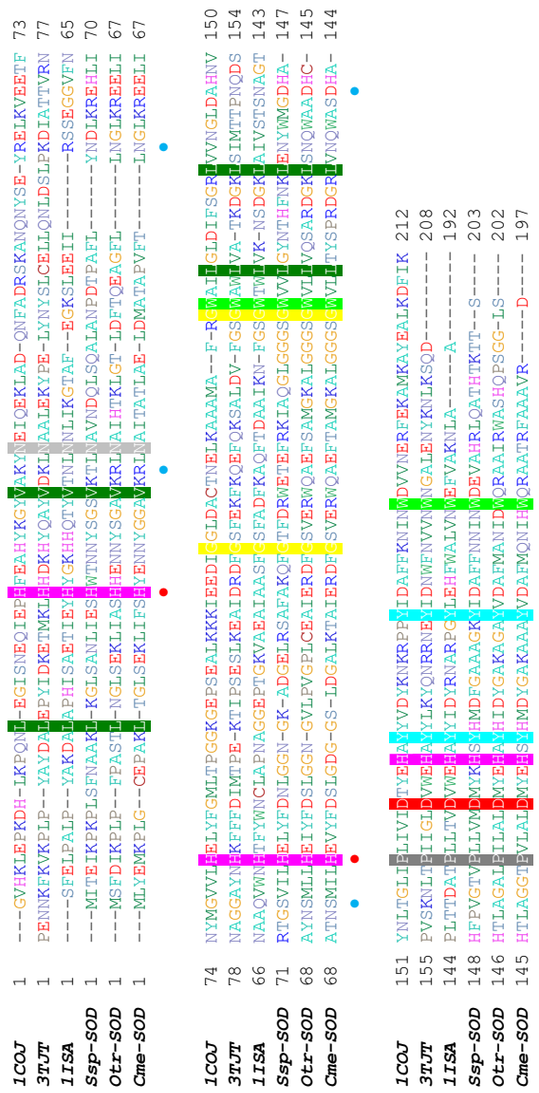

Figure 3 Sequence alignment of SOD proteins. Sequences of two SODs related to chromate resistance (ChrC) and three SODs that have been crystallised are compared. The sequences used were: Cme-SOD, SOD-ChrC from *Cupriavidus metallidurans* CH34 (accession number: CAC42412). Otr-ChrC, SOD-ChrC from *Ochrobactrum tritici* (accession number: ABO70324). Ssp-SOD, SOD-ChrC from *Shewanella* sp. ANA-3 (Accession No: WP_041413376). 1COJ, SOD from *Aquifex pyrophilus*. 3TJT, SOD of *Clostridium difficile* 630. 1ISA, SOD of *Escherichia coli*. Red ● marks the conserved residues forming the Fe-binding site. Blue ● indicates other residues forming the active site

Acknowledgements

This project was carried out thanks to funding from DCSI-University of Guanajuato, project CIDSC-2350807.

References

Aguilar, J. A., Díaz-Pérez, C., Díaz-Pérez, A. L., Rodríguez-Zavala, J. S., Nikolau, B. J., & Campos-García, J. (2008). Substrate specificity of the 3-methylcrotonyl coenzyme A (CoA) and geranyl-CoA carboxylases from *Pseudomonas aeruginosa*. *Journal of Bacteriology*, *190*(14), 4888-4893. https://doi.org/10.1128/jb.00454-08

Altschul, S. F., Madden, T. L., Schäffer, A. A., Zhang, J., Zhang, Z., Miller, W., & Lipman, D. J. (1997). Gapped BLAST and PSI-BLAST: a new generation of protein database search programs. *Nucleic acids research*, *25*(17), 3389-3402. https://doi.org/10.1093/nar/25.17.3389
Alvarez, C. C., Gómez, M. E. B., & Zavala, A. H. (2021). Hexavalent chromium: Regulation and health effects. *Journal of Trace Elements in Medicine and Biology*, *65*, 126729. https://doi.org/10.1016/j.jtemb.2021.126729

Baldiris, R., Acosta-Tapia, N., Montes, A., Hernández, J., & Vivas-Reyes, R. (2018). Reduction of hexavalent chromium and detection of chromate reductase (ChrR) in Stenotrophomonas maltophilia. *Molecules*, *23*(2), 406. https://doi.org/10.3390/molecules23020406

Branco, R., & Morais, P. V. (2016). Two superoxide dismutases from TnOtchr are involved in detoxification of reactive oxygen species induced by chromate. *BMC microbiology*, *16*(1), 1-10. https://doi.org/10.1186/s12866-016-0648-0

Dalton, J. A., & Jackson, R. M. (2010). Homology-modelling protein–ligand interactions: allowing for ligand-induced conformational change. *Journal of molecular biology*, *399*(4), 645-661. https://doi.org/10.1016/j.jmb.2010.04.047

Di Tommaso, P., Moretti, S., Xenarios, I., Orobitg, M., Montanyola, A., Chang, J.-M., Taly, J.-F., & Notredame, C. (2011). T-Coffee: a web server for the multiple sequence alignment of protein and RNA sequences using structural information and homology extension. *Nucleic acids research*, *39*(suppl_2), W13-W17. https://doi.org/10.1093/nar/gkr245

ISSN-On line: 2410-4191

Duffus, J. H. (2002). " Heavy metals" a meaningless term?(IUPAC Technical Report). *Pure and applied chemistry*, *74*(5), 793-807. https://doi.org/10.1351/pac200274050793

Houba, C. (1976). *Etude de l'influence de l'ion cadmium sur des cultures bactériennes par comparaison de souches sensibles et résistantes.* University of Liège.

Juhnke, S., Peitzsch, N., Hübener, N., Große, C., & Nies, D. H. (2002). New genes involved in chromate resistance in *Ralstonia metallidurans* strain CH34. *Archives of microbiology*, *179*, 15-25. https://doi.org/10.1007/s00203-002-0492-5

Jumper, J., Evans, R., Pritzel, A., Green, T., Figurnov, M., Ronneberger, O., Tunyasuvunakool, K., Bates, R., Žídek, A., & Potapenko, A. (2021). Highly accurate protein structure prediction with AlphaFold. *Nature*, *596*(7873), 583-589. https://doi.org/10.1038/s41586-021-03819-2

Khor, B. Y., Tye, G. J., Lim, T. S., & Choong, Y. S. (2015). General overview on structure prediction of twilight-zone proteins. *Theoretical Biology and Medical Modelling*, *12*(1), 1-11. https://10.1186/s12976-015-0014-1

Kuhlman, B., & Bradley, P. (2019). Advances in protein structure prediction and design. *Nature Reviews Molecular Cell Biology*, *20*(11), 681-697. https://doi.org/10.1038/s41580-019-0163-x

Lah, M. S., Dixon, M. M., Pattridge, K. A., Stallings, W. C., Fee, J. A., & Ludwig, M. L. (1995). Structure-function in *Escherichia coli* iron superoxide dismutase: comparisons with the manganese enzyme from *Thermus thermophilus*. *Biochemistry*, *34*(5), 1646-1660. https://doi.org/10.1021/bi00005a021

Laskowski, R. A., MacArthur, M. W., Moss, D. S., & Thornton, J. M. (1993). PROCHECK: a program to check the stereochemical quality of protein structures. *Journal of applied crystallography*, *26*(2), 283-291. https://doi.org/10.1107/S0021889892009944

Lim, J.-H., Yu, Y. G., Han, Y. S., Cho, S.-j., Ahn, B.-Y., Kim, S.-H., & Cho, Y. (1997). The crystal structure of an Fe-superoxide dismutase from the hyperthermophile *Aquifex pyrophilus* at 1.9 Å resolution: structural basis for thermostability. *Journal of molecular biology*, *270*(2), 259-274. https://doi.org/10.1006/jmbi.1997.1105

Mala, J. G. S. M., Takeuchi, S., Sujatha, D., & Mani, U. (2020). Microbial chromate reductases: novel and potent mediators in chromium bioremediation-a review. *Applied Microbiology: Theory & Technology*, 32-44. https://doi.org/10.37256/amtt.112020222

Mergeay, M., & Van Houdt, R. (2021). *Cupriavidus metallidurans* CH34, a historical perspective on its discovery, characterization and metal resistance. *FEMS Microbiology Ecology*, *97*(2), fiaa247. https://doi.org/10.1093/femsec/fiaa247

Miranda, A. T., González, M. V., González, G., Vargas, E., Campos-García, J., & Cervantes, C. (2005). Involvement of DNA helicases in chromate resistance by *Pseudomonas aeruginosa* PAO1. *Mutation Research/Fundamental and Molecular Mechanisms of Mutagenesis*, *578*(1-2), 202-209. https://doi.org/10.1016/j.mrfmmm.2005.05.018

Monsieurs, P., Hobman, J., Vandenbussche, G., Mergeay, M., & Van Houdt, R. (2015). Response of Cupriavidus metallidurans CH34 to metals. In *Metal Response in Cupriavidus metallidurans: Volume I: From Habitats to Genes and Proteins* (pp. 45-89). https://doi.org/https://doi.org/10.1007

Nanda, M., Kumar, V., & Sharma, D. (2019). Multimetal tolerance mechanisms in bacteria: The resistance strategies acquired by bacteria that can be exploited to 'clean-up'heavy metal contaminants from water. *Aquatic toxicology*, *212*, 1-10. https://doi.org/10.1016/j.aquatox.2019.04.011

Nies, D. H. (1999). Microbial heavy-metal resistance. *Appl Microbiol Biotechnol*, *51*(6), 730-750. https://doi.org/10.1007/s002530051457

ISSN-On line: 2410-4191

Nies, D. H. (2003). Efflux-mediated heavy metal resistance in prokaryotes. *FEMS Microbiol Rev*, *27*(2-3), 313-339. https://doi.org/10.1016/S0168-6445(03)00048-2

Ramírez-Díaz, M. I., Díaz-Pérez, C., Vargas, E., Riveros-Rosas, H., Campos-García, J., & Cervantes, C. (2008). Mechanisms of bacterial resistance to chromium compounds. *Biometals*, *21*(3), 321-332. https://doi.org/10.1007/s10534-007-9121-8

Sánchez-Calderón, L., Chávez-Avilés, M. N., Díaz-Pérez, A. L., Veloz-García, R. A., & Díaz-Pérez, C. (2019). Análisis estructural de la superóxido dismutasa ChrC de Ochrobactrum tritici. *Visum Mundi,*, *3*(2), 173-179.

Sheng, Y., Abreu, I. A., Cabelli, D. E., Maroney, M. J., Miller, A.-F., Teixeira, M., & Valentine, J. S. (2014). Superoxide dismutases and superoxide reductases. *Chemical reviews*, *114*(7), 3854-3918. https://doi.org/10.1021/cr4005296

Waterhouse, A., Bertoni, M., Bienert, S., Studer, G., Tauriello, G., Gumienny, R., Heer, F. T., de Beer, T. A. P., Rempfer, C., & Bordoli, L. (2018). SWISS-MODEL: homology modelling of protein structures and complexes. *Nucleic acids research*, *46*(W1), W296-W303. https://doi.org/10.1093/nar/gky427

Webb, B., & Sali, A. (2016). Comparative protein structure modeling using MODELLER. *Current protocols in bioinformatics*, *54*(1), 5.6. 1-5.6. 37. https://doi.org/10.1002/cpbi.3

Zhao, H., Zhang, R., Yan, X., & Fan, K. (2021). Superoxide dismutase nanozymes: an emerging star for anti-oxidation. *Journal of Materials Chemistry B*, *9*(35), 6939-6957. https://10.1039/D1TB00720C.

ISSN-On line: 2410-4191

Article **ECORFAN Journal-Bolivia**
June 2023, Vol.10 No.18 24-32

Nephroprotection of *p*-coumaric acid against sublethal dose of carbon tetrachloride in Wistar rats: histological evidence

Nefroprotección del ácido *p*-cumárico ante la dosis subletal de tetracloruro de carbono en rata Wistar: evidencias histológicas

MACÍAS-PÉREZ, José Roberto*†, ALDABA-MURUATO, Liseth Rubí*, HERNÁNDEZ-MARTÍNEZ, Jazmín Guadalupe and SÁNCHEZ-BRIONES, María Eugenia

Facultad de Estudios Profesionales Zona Huasteca, Universidad Autónoma de San Luis Potosí. Romualdo del Campo No. 501, Rafael Curiel, C.P. 79060, Ciudad Valles, San Luis Potosí, México

ID 1st Author: *José Roberto, Macías-Pérez* / **ORC ID:** 0000-0001-7925-2494, **Researcher ID Thomson:** X-2998-2018, **CVU CONAHCYT:** 172982.

ID 1st Co-author: *Liseth Rubí, Aldaba-Muruato* / **ORC ID:** 0000-0002-9641-662X, **Researcher ID Thomson:** X-3211-2018, **CVU CONAHCYT ID:** 176507.

ID 2nd Co-author: *Jazmín Guadalupe, Hernández-Martínez* / **ORC ID:** 0009-0004-6239-6300, Becario CONAHCYT ID: 1138163.

ID 3rd Co-author: *Sánchez-Briones María Eugenia* / **ORC ID:** 0000-0001-9968-0322, **Researcher ID Thomson:** ABE-2865-2020, **CVU CONAHCYT ID:** 265765

DOI: 10.35429/EJB.2023.18.10.24.32 Received: January 30, 2023; Accepted: June 30, 2023

Abstract

In Mexico, chronic kidney disease is a public health problem, when is diagnosed in advanced stages, the only treatment options are dialysis, hemodialysis or organ transplantation, however, the health system does not have the economic capacity or the infrastructure to fully cover these treatments. Therefore, the objective of this research work was to evaluate the activity of the *p*-coumaric acid (*p*CA) as a possible nephroprotective agent against toxic carbon tetrachloride (CCl_4)-induced kidney damage in male Wistar rats. Renal parenchyma was evaluated using two stains, hematoxylin and eosin (H&E) and periodic acid with Schiff's reagent (PAS). The administration of CCl_4 (4 g/kg, p.o., one dose) induced tubular necrosis and glomerular rupture within 24 h, with loss of microvilli and basement membranes, with widening of the lumen of the distal and proximal tubules. On the other hand, *p*CA (100 mg/kg, p.o., administered 24 h and 1 h before CCl_4 and 1 h after this toxic agent) showed nephroprotective action by reducing the presence of these morphological changes. Our results suggest for the first time that *p*CA, when administered preventively, slows the deterioration of renal structure induced by acute exposure to a sublethal dose of CCl_4.

Nephropathy, Acute kidney injury, CCl_4, *p*-coumaric acid, Nephroprotective

Resumen

En México la enfermedad renal crónica es un problema de salud pública, que tiene como opción de tratamiento la diálisis, la hemodiálisis o el trasplante de órgano, sin embargo, el sistema de salud no tiene la capacidad económica ni la infraestructura para cubrirlos en su totalidad. Por lo tanto, el objetivo del presente trabajo fue evaluar la actividad del ácido *p*-cumárico (*p*CA) como un posible agente nefroprotector contra el daño inducido con el tóxico tetracloruro de carbono (CCl_4) en las ratas Wistar macho. El parénquima renal fue evaluado mediante dos tinciones, la de hematoxilina y eosina y la del ácido peryódico de Schiff. La administración de CCl_4 (4 g/kg, p.o., una dosis) indujo en 24 h necrosis tubular y ruptura glomerular, con pérdida de microvellosidades y de membranas basales, con ensanchamiento de la luz de los túbulos distales y proximales. Por otra parte, el *p*CA (100 mg/kg, p.o., administrado 24 h y 1 h antes que el CCl_4 y 1 h después de este agente tóxico) mostró acción nefroprotectora al disminuir la presencia de estos cambios morfológicos. Nuestros resultados sugieren por primera vez que el *p*CA puede prevenir el deterioro de la estructura renal ante la exposición aguda de CCl_4.

Nefropatía, daño renal agudo, CCl_4, *ácido p*-cumárico, nefroprotector

Citation: MACÍAS-PÉREZ, José Roberto, ALDABA-MURUATO, Liseth Rubí, HERNÁNDEZ-MARTÍNEZ, Jazmín Guadalupe and SÁNCHEZ-BRIONES, María Eugenia. Nephroprotection of p-coumaric acid against sublethal dose of carbon tetrachloride in Wistar rats: histological evidence. ECORFAN-Bolivia Journal. 2023. 10-18:24-32.

* Correspondence to Author (E-mail: roberto.macias@uaslp.mx, liseth.aldaba@uaslp.mx)
† Researcher contributing as first author.

Introduction

Currently, one of the diseases that most afflict human beings are those of renal origin, with chronic kidney disease (CKD) being considered a serious public health problem both in Mexico and in the world (Evans et al., 2022; Reyna-Sevilla et al., 2022). CKD is directly related to diabetes and hypertension, however, it can be caused by other factors, from the consumption of toxic substances, autoimmune diseases, infections, obstructive problems, and congenital antecedents (Talati, 2019; Perazella, 2018; Stevens, 2018; Tecklenborg, 2018; Wyatt, 2017).

Oxidative stress is one of the main factors affecting the kidney, this occurs when the production of oxidative molecules or reactive oxygen species (ROS) exceeds the endogenous antioxidant capacity of the organism, these ROS are produced in the plasma membrane, cytoplasm, endoplasmic reticulum and mitochondria (Ho & Shirakawa, 2022). The kidney, being an organ with abundant mitochondria, becomes the main site of ROS production, which under normal conditions is regulated by the regenerative cycle of mitochondrial ROS formation and release known as ROS-induced ROS release (RIRR), which upon dysfunction of mitochondrial homeostasis ROS accumulate and are released activating cell signalling pathways leading to bioenergetic and stress alterations that cause inflammation, endothelial and vascular damage, with subsequent development of acute or chronic kidney damage (Ho & Shirakawa, 2022; Zorov, et al 2014).

P-coumaric acid (pCA) or 4-hydroxycinnamic acid is a phenolic acid that is ubiquitously distributed in plants and fungi and is a precursor of a wide range of other molecules, such as flavonoids and lignin (Combes et al., 2021: Pei et al. 2016). In addition, it has numerous applications in the pharmaceutical, cosmetics and food industries (Boo, 2019; Pei et al. 2016). Moreover, various researches have shown that pCA has important biological activities such as antioxidant, anti-inflammatory, anti-apoptotic, anti-necrotic, anti-cholestatic, amebiostatic and antimicrobial (Ayazoglu et al 2022; Daroi et al 2022; Aldaba-Muruato et al., 2021; Ojha & Patil 2019).

These aforementioned properties make it suitable to be evaluated against sublethal oral dose (per os; p.o.) of 4 g/kg of carbon tetrachloride (CCl_4) (Yoshioka et al., 2016) which at high concentrations causes oxidative damage to kidney tissue (Suzuki et al., 2015; Ozturk et al., 2003).

Methodology

Experimental animals

In this research work, male Wistar rats (Rattus norvegicus) weighing approximately 230-250 g were used and subjected to a standard diet (Nutricubos®), with free access to drinking water, and maintained at a temperature of 24°C with 50-60% relative humidity and 12-hour light-dark cycles.

Ethics

The present research work belongs to the project entitled "Evaluation of compounds with hepatoprotective activity" carried out with male Wistar rats, which was accepted by the Research Ethics Committee of the Facultad de Estudios Profesionales Zona Huasteca, UASLP. All animals received humane care based on the biosafety terms and guidelines established by this committee, as well as on the specifications dictated by the official Mexican standard (NOM-062-ZOO-1999) regarding the technical specifications for the production, care and use of laboratory animals.

Chemical compounds and reagents

The reagents used for the in vivo experimental protocol were CCl_4 (mallinckrodt), pCA (sigma), carboxymethylcellulose 0.5% (sigma), mineral oil (mystic moments). On the other hand, for haematoxylin eosin (H&E) staining, xylene (CTP Scientific), ethanol (CTP Scientific), haematoxylin (CTP Scientific), eosin (Jalmek) were used and for PAS staining, Schiff's reagent, periodic acid (CTP Scientific), Mayer's haematoxylin (CTP Scientific), xylene (CTP Scientific) and ethanol (CTP Scientific) were used.

ISSN-On line: 2410-4191

Induction of renal damage with CCl_4

The twenty experimental animals were equally divided into four groups (Figure 1). Rats in the Control group were administered mineral oil (0.5 mL/100 g, p.o.), which was used as a vehicle for CCl_4, those in the CCl_4 group were induced renal damage with a single sublethal dose of CCl_4 (4 g/kg, p. o.), and rats in the CCl_4 + pCA group were administered pCA (100 mg/kg, p.o.) on three occasions, one day before CCl_4 administration, as well as one hour before and one hour after the same intoxication. The pCA group was administered pCA in the same way as in the CCl_4 group, and instead of CCl_4 the mineral oil was administered orally (0.5 mL/100 g, p.o.), and the pCA group was administered orally (0.5 mL/100 g, p.o.), and the pCA group was administered in the same way as in the CCl_4 group).

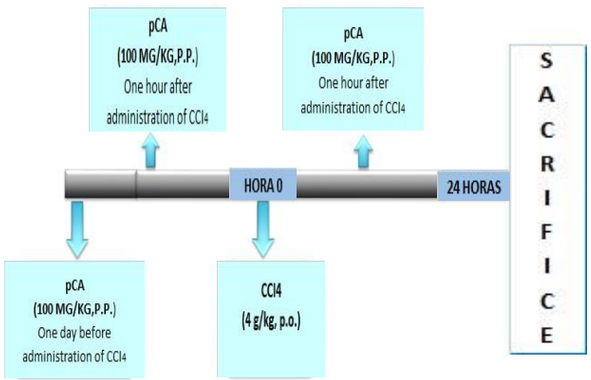

Figure 1 Experimental procedure. Twenty male Wistar rats were divided equally into four experimental groups: CCl_4 group was administered a single dose of CCl_4 (4g/kg, p.o.); animals in the CCl_4 + pCA group were administered 3 doses of pCA (each 100 mg/kg, p.o., the first two doses 24 h and 1 h before CCl_4 toxicant administration and the last dose 1 h after CCl_4). The Control group was administered only with CCl_4 and pCA vehicles (mineral oil and carboxymethylcellulose 0.5%) and the pCA group was administered in the same way as in the CCl_4 + pCA group, but instead of CCl_4, p.o. mineral oil was administered

Sacrifice

The animals were sacrificed 24 hours after CCl_4 intoxication or administration of the mineral oil. For this, the rats were first sedated with a mixture of ketamine (0.9 mL/100 g, i.p.) and xylazine (0.5 mL/100 g, i.p.), and then sacrificed by cardiac puncture.

Collection of biological samples

The left kidney was dissected out and embedded in 4% p-formaldehyde for a period of 72 h.

Paraffin-embedding of kidney tissue

After fixation, the tissues were processed with the Leica TP1020 Histochinete equipment, in order to facilitate dehydration, clarification, pre-impregnation and paraffin infiltration of the biological samples. The tissues were then immersed in paraffin to form solid blocks with the aid of MYR EC350-1 semi-automatic paraffin embedding equipment.

Histological sections

Paraffin-embedded tissue sections with a thickness of 4 µm were obtained using the Ecoshel model 202A microtome. The sections were transferred to a CA Scientific flotation bath model XH-1001 at a temperature of 40°C, and the slice was recovered with a previously silanised slide.

Haematoxylin-Eosin (H&E) staining

Dewaxing was started with xylol, 2 washes for 10 min and 1 min respectively, followed by dehydration in absolute alcohol 2 washes for 1 min, then in 96 % alcohol for 1 min, then in 80 % alcohol for 1 min and then in distilled water for 1 min. The slides were then stained with the first stain, Harris haematoxylin, in which the slides were immersed for 10 min, then washed in tap water for 5 min, immersed in acid alcohol for 15 s, placed in distilled water for 1 min, immersed in ammonia water for 1 s, then washed in distilled water for 1 min, then immersed in ammonia water for 1 min, then washed in distilled water for 1 min, then immersed in ammonia water for 1 min, washed with distilled water twice, then immersed in the second dye, eosin, for 2 min, followed by dehydration, immersed in 80% alcohol, then 96% alcohol, twice in absolute alcohol and finally with xylol, all for 1 min each. Finally, the tissue was mounted with a drop of entellan, placed on a coverslip and left to dry.

ISSN-On line: 2410-4191

Periodic acid staining with Schiff's reagent (PAS)

PAS staining began with dewaxing with xylol, 2 washes for 10 min and 1 min respectively, followed by dehydration in absolute alcohol for 2 washes for 1 min, then in 96% alcohol for 1 min, then in 80% alcohol for 1 min and then in distilled water for 1 min. The slides were placed in running water for 5 min, then in periodic acid for 5 min, at the end of this time they were placed in distilled water for 20 seconds more, and then the slides were placed in Schiff's reagent for 15 min, and then in running water for 5 min, at the end of this time the slides were placed in Schiff's reagent for 15 min, and then in running water for 5 min, at the end the slides were placed in Arris haematoxylin for 10 min, and then placed in running water for 5 min, at the end they went through the dehydration train, immersing in 80 % alcohol, then 96 % alcohol, twice in absolute alcohol and finally with xylol 2 times, all these for 1 minute each.

Photographic images

Images were taken with a KOPPACE 16 MP camera (KP-1660) adapted to an Axiostar plus (HBO 50/AC, ZEISS) brightfield microscope, which were processed and analysed in S-Eye (1.6.0.11) and ImageJ (Version: 1.52) software, respectively.

Results

The pCA is able to prevent CCl_4-induced renal damage: histopathology with H&E.

Renal architecture was assessed by H&E staining and representative images are shown at 5x (Figure 2), 10x (Figure 3) and 40x (Figure 4) magnification. Figures 2 and 3 show the main morphological changes observed at the level of the renal cortex. The Control and pCA groups showed a mostly preserved morphology with normal appearing glomeruli and distal and contoured tubules and tubules, although some glomeruli with slight morphological changes were visible. The CCl_4 group showed marked damage to the renal architecture, with evident tubular necrosis, with mostly collapsed or fragmented glomeruli.

The CCl_4 + pCA group preserved the integrity of the renal parenchyma, with the presence of mostly normal glomeruli, with occasional altered glomeruli, and the renal tubules showing an architecture with a typical appearance.

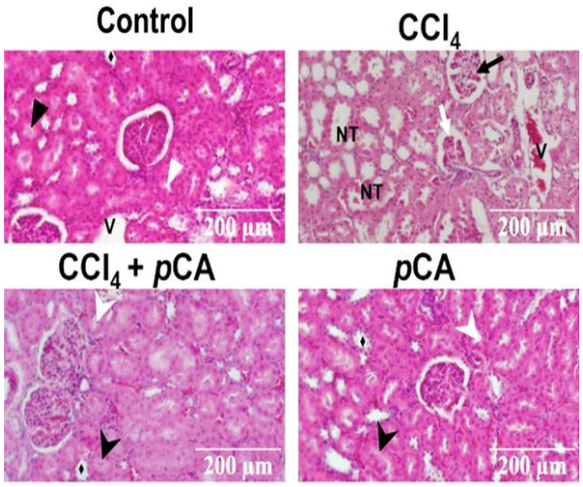

Figure 2 Representative photomicrographs at 5x of renal cortex sections stained with H&E. Experimental groups: Control (healthy group), CCl_4 (damage control), CCl_4 + pCA (test group) and pCA (pCA control). Black arrows: glomeruli with morphological alterations; White arrow: collapsed glomerulus; Glomerular rupture: (*); Tubular necrosis: NT; Artery: A; Vein: V.

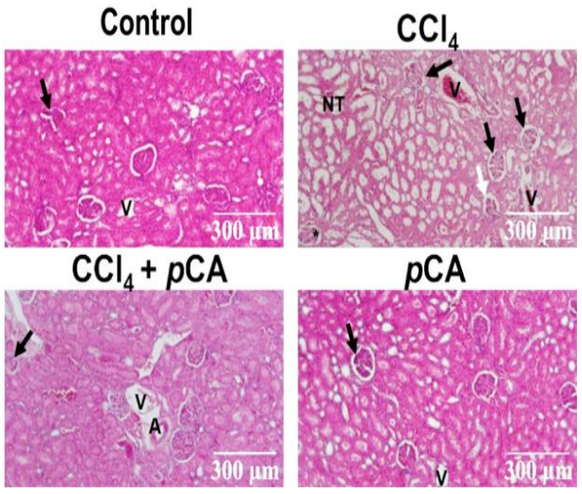

Figure 3. Representative 10x photomicrographs of renal cortex sections stained with H&E. Experimental groups: Control (healthy group), CCl_4 (damage control), CCl_4 + pCA (test group) and pCA (pCA control). Black arrowhead: proximal convoluted tubules; white arrowhead: distal convoluted tubules; black arrow: damaged glomeruli with presence of fragmentation and a wide glomerular space; white arrow: glomerular rupture and collapse; tubular necrosis: TN; loops of Henle; tubular necrosis: NT; and white arrow: glomerular rupture and collapse: (⧫).

ISSN-On line: 2410-4191

Photomicrographs at 40x magnification showed that in the healthy groups (Control and pCA) the kidneys have a normal cellular structure, with intact glomeruli (Figure 4A and B) and regular tubular contour (Figures 4A, B and C). On the other hand, glomerular atrophy (Figures 4D and E) as well as tubular destruction was observed in the CCl_4-intoxicated groups (Figures 4D, E and F), compared to the integrity shown by the healthy groups. The CCl_4 + pCA group largely prevented CCl_4-induced renal damage, the glomeruli show apparently normal morphology (Figure 4G), although it is possible to observe some glomeruli with abnormal architecture (Figure 4H), and overall the tubular morphology appears normal (Figures 4G, H and I). The pCA group showed similarities to the Control group (Figures 4J, K and L).

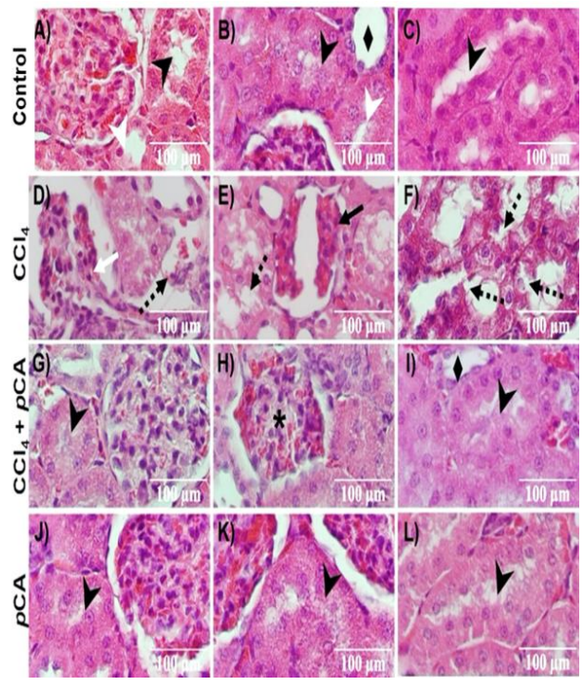

Figure 4 Representative photomicrographs at 40x of renal cortex sections stained with H&E. Experimental groups: Control (healthy group), CCl_4 (damage control), CCl_4 + pCA (test group) and pCA (pCA control). Head of black arrows: proximal convoluted tubules; Head of white arrows: distal convoluted tubules; White arrow: damaged glomeruli with presence of fragmentation and a wide glomerular space; Black arrow: glomerular collapse and rupture; Dotted black arrows: rupture of distal and proximal tubules; Loops of Henle: (⧫); Damaged glomerulus: (*)

pCA protects the integrity of the convoluted tubules: histopathology with PAS

PAS staining is used to investigate the morphological structure of the renal parenchyma, but it also allows us to correlate with the content and integrity of carbohydrates present both in the basement membrane and in the microvilli of all the epithelia and connective tissue. This gives us an idea of the condition of the convoluted tubules and whether there is damage or not.

Microscopic observations of renal tissue stained with PAS at magnifications of 5x, 10x, 40x

Observations by light microscopy at 5x (Figure 5), 10x (Figure 6) and PAS staining allowed us to evaluate the renal tubular architecture and the integrity of the basement membranes. Thus, it was possible to visualise that the healthy groups (Control and pCA) presented a normal histology, with preserved basement membrane structures, as well as the microvilli of the proximal tubules. CCl_4 intoxication induced tubular necrosis, showing loss of basement membrane and microvilli. The CCl_4 + pCA group showed a preserved architecture, preventing the loss of glomerular mass, proximal and distal tubules and microvilli.

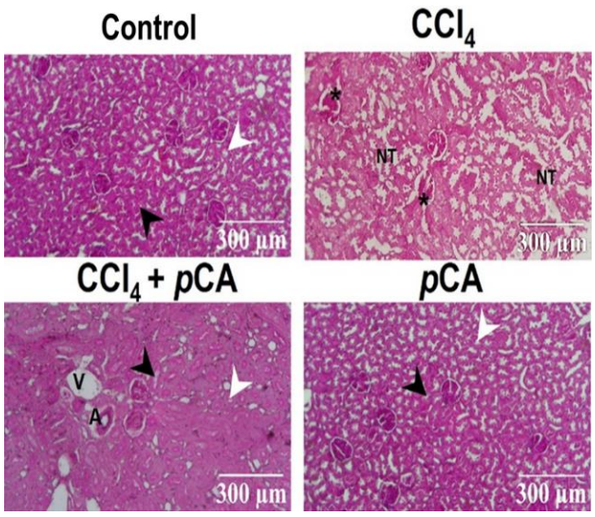

Figure 5 Representative 5x photomicrographs of PAS-stained renal cortex sections. Experimental groups: control (healthy group), CCl_4 (damage control), CCl_4 + pCA (test group) and pCA (pCA control). Head of black arrows: proximal convoluted tubules; Head of white arrows: distal convoluted tubules; Tubular necrosis: NT; glomerular rupture (*); Artery: A; Vein: V

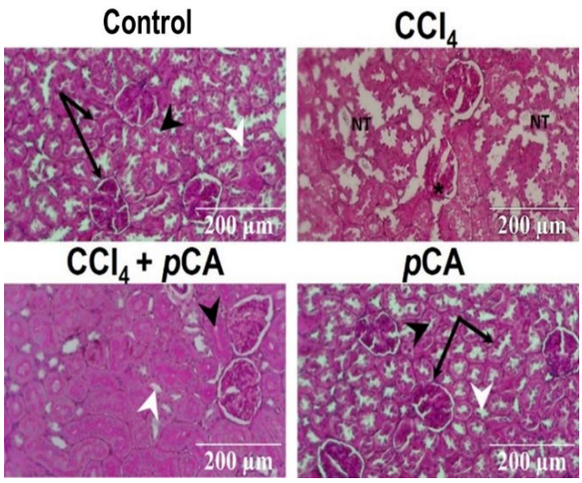

Figure 6 Representative 10x photomicrographs of PAS-stained renal cortex sections at 10x. Experimental groups: Control (healthy group), CCl_4 (damage control), CCl_4 + pCA (test group) and pCA (pCA control). Head of black arrows: proximal convoluted tubules; Head of white arrows: distal convoluted tubules; Black arrows: intact basement membranes; Tubular necrosis: NT; atrophied glomeruli: (*)

The photomicrographs at 40x magnification (Figure 7), show that the CCl_4 group presented tubular destruction with loss of microvilli and basement membrane, widening of the lumen of the distal and proximal tubules was observed in comparison with the integrity shown by the healthy groups (Mineral Ac. and pCA). The CCl_4 + pCA group prevented these morphological changes due to CCl_4-induced renal damage.

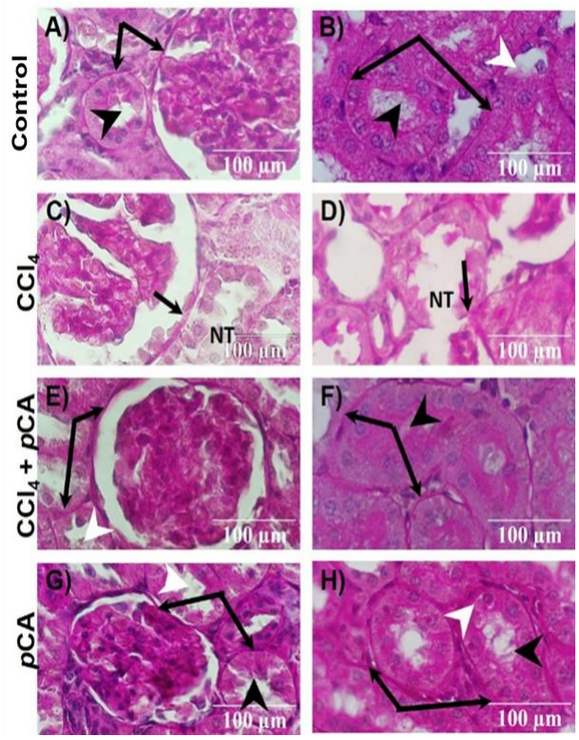

Figure 7 Representative photomicrographs at 40x of PAS-stained renal cortex sections. Experimental groups: Control (healthy group), CCl_4 (damage control), CCl_4 + pCA (test group) and pCA (pCA control). Head of black arrows: proximal convoluted tubules; Head of white arrows: distal convoluted tubules; Black arrows: basement membrane; Tubular necrosis: NT

Discussion

Prevention or early detection of kidney diseases are considered the best strategies to avoid CKD, because when CKD is already established, the patient's life expectancy decreases, as persistent urinary abnormalities with impaired nephron function occur (Romagnani et al., 2017). Therefore, in the present work, the ability of pCA as a preventive agent against acute damage induced with a sublethal dose of CCl_4 in Wistar rats was evaluated, considering that CCl_4 is a potent nephrotoxic agent (Suzuki et al., 2015; Ozturk et al., 2003).

ISSN-On line: 2410-4191

In H&E and PAS stained kidney sections, it was observed that the healthy groups (Control and pCA) which were administered mineral oil+CMC 0. 5% or mineral oil+pCA, respectively, presented a normal appearing renal parenchyma, with tissue morphology similar to a healthy kidney, with intact basement membranes, with intact glomeruli and convoluted tubules, with visibly normal cytoplasm and nuclei, however, in these healthy groups some lesions were also evident in some glomeruli and in distal and proximal convoluted tubules. These observations are related to some works that have described that olive oil which is used as a vehicle for CCl_4 induces severe renal lesions, with the presence of atrophy and destruction in the glomerulus with the presence of pyknotic nuclei and cellular infiltration (Alsalam, 2016). Therefore, our results support the fact that mineral oil has harmful effects at the renal level. Furthermore, it should be emphasised that the pCA group did not show additional morphological changes relative to the Control group.

On the other hand, CCl_4 is a chlorinated hydrocarbon composed of a mixture of chlorine with chloroform, named tetrachloromethane by the International Union of Pure and Applied Chemistry Nomenclature (IUPAC), and is highly harmful when ingested, inhaled, or by direct contact with the skin (Al Amin & Menezes, 2020). This toxic agent causes damage to multiple organs, with the liver and kidney being mainly affected; in the liver it induces necrosis, steatosis and cirrhosis and at the renal level it causes glomerular necrosis and histological alterations in distal tubules (Suzuki et al., 2015; Aldaba-Muruato et al. 2012; Ozturk et al., 2003).

A previous work published by our research group showed for the first time that pCA has anti-necrotic and anti-cholestatic activity against acute damage induced by CCl_4 or common bile duct ligation in rats, as well as amebiostatic activity against the parasite *Entamoeba histolytica* (Aldaba-Muruato et al., 2021).

The results of the present work demonstrate that pCA possesses anti-nephrotic activity at a sublethal dose of CCl_4. On the one hand, it was confirmed that CCl_4 is able to induce drastic changes in renal architecture, such as glomerular atrophy and partial or total destruction of the convoluted tubules, known as tubular necrosis (Figures 2, 3 and 4), observations consistent with other authors (Suzuki et al., 2015; Ozturk et al., 2003). On the other hand, our H&E and PAS-stained renal histopathological studies indicate that pCA possesses the ability to protect against CCl_4-induced nephrotoxic damage, with a visible reduction in cell damage, with relative integrity of the proximal convoluted tubule, as well as its visible cytoplasm and nuclei with no apparent alterations (Figures 2, 3 and 4). The PAS technique was useful to demonstrate the integrity or morphological alterations of the basement membrane of the convoluted tubules and glomeruli (Ochoa et al., 1957; Sugai et al., 1992). Similarly, microscopic observations of PAS-stained kidney sections showed that in the CCl_4 group, there is loss of basement membrane continuity of the different structures of the nephron, as well as of the microvilli of proximal convoluted tubules, while these structures are more preserved in the CCl_4 + pCA group. These results are consistent with previous observations describing that pCA protects against tubular necrosis by preventing the production of oxidative stress that is generated by cisplatin (Ekinci et al 2017). Likewise, Gentamicin-induced tubular necrosis and tubulointerstitial inflammation of the proximal tubules was reduced by pCA (Hakyemez et al 2022). In addition, another work demonstrated that the antioxidant effect of pCA reduces oxidative stress induced in diabetic rats and prevents the development of diabetes-associated nephropathy (Mani, et al., 2022).

Conclusion

The present work demonstrates that pCA is a potent nephroprotectant against renal damage induced by sublethal doses of CCl_4.

Funding

The authors are grateful to CONAHCYT for funding No. 320331 "Basic and/or Frontier Science Modality: Paradigms and Controversies of Science 2022".

ISSN-On line: 2410-4191

References

Al Amin, A. S. M., & Menezes, R. G. (2023). Carbon Tetrachloride Toxicity. In *StatPearls*. StatPearls Publishing. Available from: https://www.ncbi.nlm.nih.gov/books/NBK562180/

Aldaba-Muruato, L. R., Moreno, M. G., Shibayama, M., Tsutsumi, V., & Muriel, P. (2012). Protective effects of allopurinol against acute liver damage and cirrhosis induced by carbon tetrachloride: modulation of NF-κB, cytokine production and oxidative stress. *Biochimica et biophysica acta*, *1820*(2), 65–75. https://doi.org/10.1016/j.bbagen.2011.09.018

Aldaba-Muruato, L.R., Ventura-Juárez, J., Perez-Hernandez, A.M., Hernández-Morales, A., Muñoz-Ortega, M.H., Martínez-Hernández, S.L. ... Macías-Pérez, J.R. (2021). Therapeutic perspectives of p-coumaric acid: Anti-necrotic, anti-cholestatic and anti-amoebic activities. World Academy of Sciences Journal, 3, 47. https://doi.org/10.3892/wasj.2021.118

Alsalam Ali Abd, Elshaer Fathy M., Mansour Hamdi Abdou. 2016. Assessment of the Potential role of Hesperidin as an Antioxidant on the Carbon Tetrachloride -Induced Kidney Damage in Rats. The Egyptian Journal of Hospital Medicine. 64: 277-286. Recuperado de https://journals.ekb.eg/article_15141_4281e11f3f4058ba9bb22abf634bab6c.pdf

Ayazoglu Demir, E., Mentese, A., Kucuk, H., Turkmen Alemdar, N., & Demir, S. (2022). p-Coumaric acid alleviates cisplatin-induced ovarian toxicity in rats. The journal of obstetrics and gynaecology research, 48(2), 411–419. https://doi.org/10.1111/jog.15119

Boo Y. C. (2019). p-Coumaric Acid as An Active Ingredient in Cosmetics: A Review Focusing on its Antimelanogenic Effects. Antioxidants (Basel, Switzerland), 8(8), 275. https://doi.org/10.3390/antiox8080275

Combes, J., Imatoukene, N., Couvreur, J., Godon, B., Brunissen, F., Fojcik, C., Allais, F., & Lopez, M. (2021). Intensification of p-coumaric acid heterologous production using extractive biphasic fermentation. Bioresource technology, 337, 125436. https://doi.org/10.1016/j.biortech.2021.125436

Daroi, P. A., Dhage, S. N., & Juvekar, A. R. (2022). p-Coumaric acid mitigates lipopolysaccharide induced brain damage via alleviating oxidative stress, inflammation and apoptosis. The Journal of pharmacy and pharmacology, 74(4), 556–564. https://doi.org/10.1093/jpp/rgab077

Ekinci Akdemir, F. N., Albayrak, M., Çalik, M., Bayir, Y., & Gülçin, İ. (2017). The Protective Effects of p-Coumaric Acid on Acute Liver and Kidney Damages Induced by Cisplatin. Biomedicines, 5(2), 18. https://doi.org/10.3390/biomedicines5020018

Evans, M., Lewis, R. D., Morgan, A. R., Whyte, M. B., Hanif, W., Bain, S. C., Davies, S., Dashora, U., Yousef, Z., Patel, D. C., & Strain, W. D. (2022). A Narrative Review of Chronic Kidney Disease in Clinical Practice: Current Challenges and Future Perspectives. Advances in therapy, 39(1), 33–43. https://doi.org/10.1007/s12325-021-01927-z

Hakyemez, I. N., Cevizci, M. N., Aksoz, E., Yilmaz, K., Uysal, S., & Altun, E. (2022). Protective effects of p-coumaric acid against gentamicin-induced nephrotoxicity in rats. Drug and chemical toxicology, 45(6), 2825–2832. https://doi.org/10.1080/01480545.2021.1993703

Ho, H. J., & Shirakawa, H. (2022). Oxidative Stress and Mitochondrial Dysfunction in Chronic Kidney Disease. Cells, 12(1), 88. https://doi.org/10.3390/cells12010088

Mani, A., Kushwaha, K., Khurana, N., & Gupta, J. (2022). p-Coumaric acid attenuates high-fat diet-induced oxidative stress and nephropathy in diabetic rats. Journal of animal physiology and animal nutrition, 106(4), 872–880. https://doi.org/10.1111/jpn.13645

Ochoa PC, Smith OD, Swerdlow M. "The Dermal-Eepidermal Junction; A Preliminary Study with Periodic Acid-Schiff Stain". AMA Arch Dermatol 1957; 75(1): 70-77. doi:10.1001/archderm.1957.01550130072007

ISSN-On line: 2410-4191

Ojha, D., & Patil, K. N. (2019). p-Coumaric acid inhibits the Listeria monocytogenes RecA protein functions and SOS response: An antimicrobial target. Biochemical and biophysical research communications, 517(4), 655–661. https://doi.org/10.1016/j.bbrc.2019.07.093

Ozturk, F., Ucar, M., Ozturk, I. C., Vardi, N., & Batcioglu, K. (2003). Carbon tetrachloride-induced nephrotoxicity and protective effect of betaine in Sprague-Dawley rats. *Urology*, *62*(2), 353–356. https://doi.org/10.1016/s0090-4295(03)00255-3

Pei, K., Ou, J., Huang, J., & Ou, S. (2016). p-Coumaric acid and its conjugates: dietary sources, pharmacokinetic properties and biological activities. Journal of the science of food and agriculture, 96(9), 2952–2962. https://doi.org/10.1002/jsfa.7578

Perazella M. A. (2018). Pharmacology behind Common Drug Nephrotoxicities. Clinical journal of the American Society of Nephrology: CJASN, 13(12), 1897–1908. https://doi.org/10.2215/CJN.00150118

Reyna-Sevilla A, Borrayo-Sánchez G, Duque-Molina C, Ascencio-Montiel IJ, Torres-Toledano M. Análisis geográfico de nefropatía diabética e insuficiencia renal en el primer nivel de atención IMSS 2019. Rev Med Ins Mex Seguro Soc. 2022; 60(2): 156-163. https://www.ncbi.nlm.nih.gov/pmc/articles/PMC10395952/?report=reader

Romagnani, P., Remuzzi, G., Glassock, R., Levin, A., Jager, K. J., Tonelli, M., Massy, Z., Wanner, C., & Anders, H. J. (2017). Chronic kidney disease. Nature reviews. Disease primers, 3, 17088. https://doi.org/10.1038/nrdp.2017.88

Stevens S. (2018). Obstructive Kidney Disease. The Nursing clinics of North America, 53(4), 569–578. https://doi.org/10.1016/j.cnur.2018.07.007

Sugai SA, Gerbase AB, Cernea SS, Sotto MN, Oliveira ZN, Vilela MA, Rivitti EA, Miyauchi LM, Sampaio SA. "Cutaneous Lupus Erythematosus: Direct immunofluorescence and Epidermal Basal Membrane Study". Int J Dermatol 1992; 31(4): 260-264. https://doi.org/10.1111/j.1365-4362.1992.tb03567.x

Suzuki, K., Nakagawa, K., Yamamoto, T., Miyazawa, T., Kimura, F., Kamei, M., & Miyazawa, T. (2015). Carbon tetrachloride-induced hepatic and renal damages in rat: inhibitory effects of cacao polyphenol. Bioscience, biotechnology, and biochemistry, 79(10), 1669–1675. https://doi.org/10.1080/09168451.2015.1039481

Talati, A. N., Webster, C. M., & Vora, N. L. (2019). Prenatal genetic considerations of congenital anomalies of the kidney and urinary tract (CAKUT). Prenatal diagnosis, 39(9), 679–692. https://doi.org/10.1002/pd.5536

Tecklenborg, J., Clayton, D., Siebert, S., & Coley, S. M. (2018). The role of the immune system in kidney disease. Clinical and experimental immunology, 192(2), 142–150. https://doi.org/10.1111/cei.13119

Yoshioka, H., Usuda, H., Nonogaki, T., & Onosaka, S. (2016). Carbon tetrachloride-induced lethality in mouse is prevented by multiple pretreatment with zinc sulfate. The Journal of toxicological sciences, 41(1), 55–63. https://doi.org/10.2131/jts.41.55

Wyatt C. M. (2017). Kidney Disease and HIV Infection. Topics in antiviral medicine, 25(1), 13–16. https://www.ncbi.nlm.nih.gov/pmc/articles/PMC5677039/?report=reader

Zorov, D. B., Juhaszova, M., & Sollott, S. J. (2014). Mitochondrial reactive oxygen species (ROS) and ROS-induced ROS release. Physiological reviews, 94(3), 909–950. https://doi.org/10.1152/physrev.00026.2013

ISSN-On line: 2410-4191

[Title in Times New Roman and Bold No. 14 in English and Spanish]

Surname (IN UPPERCASE), Name 1st Author†*, Surname (IN UPPERCASE), Name 1st Coauthor, Surname (IN UPPERCASE), Name 2nd Coauthor and Surname (IN UPPERCASE), Name 3rd Coauthor

Institutional Affiliation of Author including Dependency (No.10 Times New Roman and Italic)

International Identification of Science - Technology and Innovation

ID 1st Author: (ORC ID - Researcher ID Thomson, arXiv Author ID - PubMed Author ID - Open ID) and CVU 1st author: (Scholar-PNPC or SNI-CONAHCYT) (No.10 Times New Roman)

ID 1st Co-author: (ORC ID - Researcher ID Thomson, arXiv Author ID - PubMed Author ID - Open ID) and CVU 1st co-author: (Scholar or SNI-CONAHCYT) (No.10 Times New Roman)

ID 2nd Co-author: (ORC ID - Researcher ID Thomson, arXiv Author ID - PubMed Author ID - Open ID) and CVU 2nd co-author: (Scholar or SNI-CONAHCYT) (No.10 Times New Roman)

ID 3rd Co-author: (ORC ID - Researcher ID Thomson, arXiv Author ID - PubMed Author ID - Open ID) and CVU 3rd co-author: (Scholar or SNI-CONAHCYT) (No.10 Times New Roman)

(Report Submission Date: Month, Day, and Year); Accepted (Insert date of Acceptance: Use Only ECORFAN)

Abstract (In English, 150-200 words)

Objectives
Methodology
Contribution

Abstract (In Spanish, 150-200 words)

Objectives
Methodology
Contribution

Keywords (In English)

Indicate 3 keywords in Times New Roman and Bold No. 10

Keywords (In Spanish)

Indicate 3 keywords in Times New Roman and Bold No. 10

Citation: Surname (IN UPPERCASE), Name 1st Author, Surname (IN UPPERCASE), Name 1st Co-author, Surname (IN UPPERCASE), Name 2nd Co-author and Surname (IN UPPERCASE), Name 3rd Co-author. Paper Title. ECORFAN Journal-Bolivia. Year 1-1: 1-11 [Times New Roman No.10]

* Correspondence to Author (example@example.org)
† Researcher contributing as first author.

Introduction

Text in Times New Roman No.12, single space.

General explanation of the subject and explain why it is important.

What is your added value with respect to other techniques?

Clearly focus each of its features

Clearly explain the problem to be solved and the central hypothesis.

Explanation of sections Article.

Development of headings and subheadings of the article with subsequent numbers

[Title No.12 in Times New Roman, single spaced and bold]

Products in development No.12 Times New Roman, single spaced.

Including graphs, figures and tables-Editable

In the article content any graphic, table and figure should be editable formats that can change size, type and number of letter, for the purposes of edition, these must be high quality, not pixelated and should be noticeable even reducing image scale.

[Indicating the title at the bottom with No.10 and Times New Roman Bold]

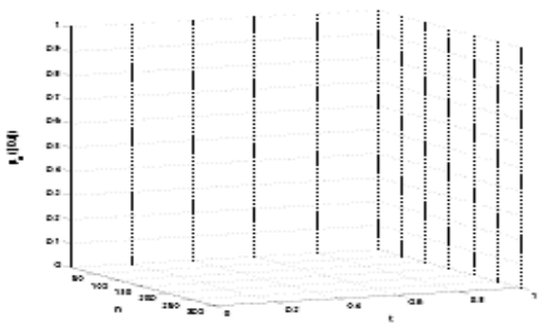

Graphic 1 Title and *Source (in italics)*

Should not be images-everything must be editable.

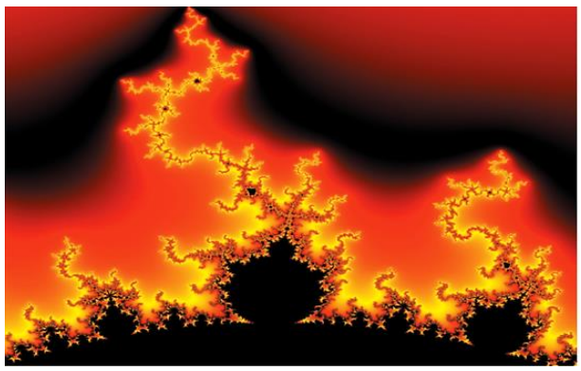

Figure 1 Title and *Source (in italics)*

Should not be images-everything must be editable.

Table 1 Title and *Source (in italics)*

Should not be images-everything must be editable.

Each article shall present separately in **3 folders**: a) Figures, b) Charts and c) Tables in .JPG format, indicating the number and sequential Bold Title.

For the use of equations, noted as follows:

$$Y_{ij} = \alpha + \sum_{h=1}^{r} \beta_h X_{hij} + u_j + e_{ij} \quad (1)$$

Must be editable and number aligned on the right side.

Methodology

Develop give the meaning of the variables in linear writing and important is the comparison of the used criteria.

Results

The results shall be by section of the article.

Annexes

Tables and adequate sources

Thanks

Indicate if they were financed by any institution, University or company.

ISSN 2410-4191

Conclusions

Explain clearly the results and possibilities of improvement.

References

Use APA system. Should not be numbered, nor with bullets, however if necessary numbering will be because reference or mention is made somewhere in the Article.

Use Roman Alphabet, all references you have used must be in the Roman Alphabet, even if you have quoted an Article, book in any of the official languages of the United Nations (English, French, German, Chinese, Russian, Portuguese, Italian, Spanish, Arabic), you must write the reference in Roman script and not in any of the official languages.

Technical Specifications

Each article must submit your dates into a Word document (.docx):

Journal Name
Article title
Abstract
Keywords
Article sections, for example:

1. Introduction
2. Description of the method
3. Analysis from the regression demand curve
4. Results
5. Thanks
6. Conclusions
7. References

Author Name (s)
Email Correspondence to Author
References

Intellectual Property Requirements for editing:

- Authentic Signature in Color of Originality Format Author and Coauthors.
- Authentic Signature in Color of the Acceptance Format of Author and Coauthors.
- Authentic Signature in blue colour of the Conflict of Interest Format of Author and Co-authors.

ISSN 2410-4191

Reservation to Editorial Policy

ECORFAN-Journal Bolivia reserves the right to make editorial changes required to adapt the Articles to the Editorial Policy of the Journal. Once the Article is accepted in its final version, the Journal will send the author the proofs for review. ECORFAN® will only accept the correction of errata and errors or omissions arising from the editing process of the Journal, reserving in full the copyrights and content dissemination. No deletions, substitutions or additions that alter the formation of the Article will be accepted.

Code of Ethics - Good Practices and Declaration of Solution to Editorial Conflicts

Declaration of Originality and unpublished character of the Article, of Authors, on the obtaining of data and interpretation of results, Acknowledgments, Conflict of interests, Assignment of rights and Distribution.

The ECORFAN-Mexico, S.C Management claims to Authors of Articles that its content must be original, unpublished and of Scientific, Technological and Innovation content to be submitted for evaluation.

The Authors signing the Article must be the same that have contributed to its conception, realization and development, as well as obtaining the data, interpreting the results, drafting and reviewing it. The Corresponding Author of the proposed Article will request the form that follows.

Article title:

– The sending of an Article to ECORFAN -Journal Bolivia emanates the commitment of the author not to submit it simultaneously to the consideration of other series publications for it must complement the Format of Originality for its Article, unless it is rejected by the Arbitration Committee, it may be withdrawn.

– None of the data presented in this article has been plagiarized or invented. The original data are clearly distinguished from those already published. And it is known of the test in PLAGSCAN if a level of plagiarism is detected Positive will not proceed to arbitrate.

– References are cited on which the information contained in the Article is based, as well as theories and data from other previously published Articles.

– The authors sign the Format of Authorization for their Article to be disseminated by means that ECORFAN-Mexico, S.C. In its Holding Bolivia considers pertinent for disclosure and diffusion of its Article its Rights of Work.

– Consent has been obtained from those who have contributed unpublished data obtained through verbal or written communication, and such communication and Authorship are adequately identified.

– The Author and Co-Authors who sign this work have participated in its planning, design and execution, as well as in the interpretation of the results. They also critically reviewed the paper, approved its final version and agreed with its publication.

– No signature responsible for the work has been omitted and the criteria of Scientific Authorization are satisfied.

– The results of this Article have been interpreted objectively. Any results contrary to the point of view of those who sign are exposed and discussed in the Article.

Copyright and Access

The publication of this Article supposes the transfer of the copyright to ECORFAN-Mexico, SC in its Holding Bolivia for its ECORFAN-Journal Bolivia, which reserves the right to distribute on the Web the published version of the Article and the making available of the Article in This format supposes for its Authors the fulfilment of what is established in the Law of Science and Technology of the United Mexican States, regarding the obligation to allow access to the results of Scientific Research.

Article Title:

Name and Surnames of the Contact Author and the Co-authors	Signature
1.	
2.	
3.	
4.	

Principles of Ethics and Declaration of Solution to Editorial Conflicts

Editor Responsibilities

The Publisher undertakes to guarantee the confidentiality of the evaluation process, it may not disclose to the Arbitrators the identity of the Authors, nor may it reveal the identity of the Arbitrators at any time.

The Editor assumes the responsibility to properly inform the Author of the stage of the editorial process in which the text is sent, as well as the resolutions of Double-Blind Review.

The Editor should evaluate manuscripts and their intellectual content without distinction of race, gender, sexual orientation, religious beliefs, ethnicity, nationality, or the political philosophy of the Authors.

The Editor and his editing team of ECORFAN® Holdings will not disclose any information about Articles submitted to anyone other than the corresponding Author.

The Editor should make fair and impartial decisions and ensure a fair Double-Blind Review.

Responsibilities of the Editorial Board

The description of the peer review processes is made known by the Editorial Board in order that the Authors know what the evaluation criteria are and will always be willing to justify any controversy in the evaluation process. In case of Plagiarism Detection to the Article the Committee notifies the Authors for Violation to the Right of Scientific, Technological and Innovation Authorization.

Responsibilities of the Arbitration Committee

The Arbitrators undertake to notify about any unethical conduct by the Authors and to indicate all the information that may be reason to reject the publication of the Articles. In addition, they must undertake to keep confidential information related to the Articles they evaluate.

Any manuscript received for your arbitration must be treated as confidential, should not be displayed or discussed with other experts, except with the permission of the Editor.

The Arbitrators must be conducted objectively, any personal criticism of the Author is inappropriate.

The Arbitrators must express their points of view with clarity and with valid arguments that contribute to the Scientific, Technological and Innovation of the Author.

The Arbitrators should not evaluate manuscripts in which they have conflicts of interest and have been notified to the Editor before submitting the Article for Double-Blind Review.

Responsibilities of the Authors

Authors must guarantee that their articles are the product of their original work and that the data has been obtained ethically.

Authors must ensure that they have not been previously published or that they are not considered in another serial publication.

Authors must strictly follow the rules for the publication of Defined Articles by the Editorial Board.

The authors have requested that the text in all its forms be an unethical editorial behavior and is unacceptable, consequently, any manuscript that incurs in plagiarism is eliminated and not considered for publication.

Authors should cite publications that have been influential in the nature of the Article submitted to arbitration.

Information services

Indexation - Bases and Repositories

LATINDEX (Scientific Journals of Latin America, Spain and Portugal)
RESEARCH GATE (Germany)
GOOGLE SCHOLAR (Citation indices-Google)
REDIB (Ibero-American Network of Innovation and Scientific Knowledge- CSIC)
MENDELEY (Bibliographic References Manager)

Publishing Services

Citation and Index Identification H
Management of Originality Format and Authorization
Testing Article with PLAGSCAN
Article Evaluation
Certificate of Double-Blind Review
Article Edition
Web layout
Indexing and Repository
ArticleTranslation
Article Publication
Certificate of Article
Service Billing

Editorial Policy and Management

21 Santa Lucía, CP-5220. Libertadores -Sucre–Bolivia. Phones: +52 1 55 6159 2296, +52 1 55 1260 0355, +52 1 55 6034 9181; Email: contact@ecorfan.org www.ecorfan.org

ECORFAN Journal-Bolivia

2410 4191
ISSN 2410-4191

www.ecorfan.org